

# β3 integrin–mediated spreading induced by matrix-bound BMP-2 controls Smad signaling in a stiffness-independent manner

Laure Fourel, Anne Valat, Eva Faurobert, Raphaël Guillot, Ingrid Bourrin-Reynard, Kefeng Ren, Laurence Lafanechère, Emmanuelle Planus, Catherine Picart, Corinne Albiges-Rizo

▶ **To cite this version:**

Laure Fourel, Anne Valat, Eva Faurobert, Raphaël Guillot, Ingrid Bourrin-Reynard, et al.. β3 integrin–mediated spreading induced by matrix-bound BMP-2 controls Smad signaling in a stiffness-independent manner. Journal of Cell Biology, 2016, 212 (6), pp.693-706. 10.1083/jcb.201508018 . hal-02324366

**HAL Id: hal-02324366**
**https://hal.science/hal-02324366**

Submitted on 21 Oct 2019

**HAL** is a multi-disciplinary open access archive for the deposit and dissemination of scientific research documents, whether they are published or not. The documents may come from teaching and research institutions in France or abroad, or from public or private research centers.

L'archive ouverte pluridisciplinaire **HAL**, est destinée au dépôt et à la diffusion de documents scientifiques de niveau recherche, publiés ou non, émanant des établissements d'enseignement et de recherche français ou étrangers, des laboratoires publics ou privés.

Published March 7, 2016



# β3 integrin–mediated spreading induced by matrix-bound BMP-2 controls Smad signaling in a stiffness-independent manner

Laure Fourel,[1,2,3,4] Anne Valat,[1,2,3,4] Eva Faurobert,[1,2,3] Raphael Guillot,[4] Ingrid Bourrin-Reynard,[1,2,3] Kefeng Ren,[4] Laurence Lafanechère,[1,3] Emmanuelle Planus,[1,2,3] Catherine Picart,[4] and Corinne Albiges-Rizo[1,2,3]

[1]Institut National de la Santé et de la Recherche Médicale U823, Institut Albert Bonniot, 38042 Grenoble, France
[2]Centre National de la Recherche Scientifique, Equipe de Recherche Labellisée 5284, 38042 Grenoble, France
[3]Université Grenoble Alpes, 38041 Grenoble, France
[4]Centre National de la Recherche Scientifique UMR 5628, Laboratoire des Matériaux et du Génie Physique, Institute of Technology, 38016 Grenoble, France

Understanding how cells integrate multiple signaling pathways to achieve specific cell differentiation is a challenging question in cell biology. We have explored the physiological presentation of BMP-2 by using a biomaterial that harbors tunable mechanical properties to promote localized BMP-2 signaling. We show that matrix-bound BMP-2 is sufficient to induce β3 integrin–dependent C2C12 cell spreading by overriding the soft signal of the biomaterial and impacting actin organization and adhesion site dynamics. In turn, αvβ3 integrin is required to mediate BMP-2–induced Smad signaling through a Cdc42–Src–FAK–ILK pathway. β3 integrin regulates a multistep process to control first BMP-2 receptor activity and second the inhibitory role of GSK3 on Smad signaling. Overall, our results show that BMP receptors and β3 integrin work together to control Smad signaling and tensional homeostasis, thereby coupling cell adhesion and fate commitment, two fundamental aspects of developmental biology and regenerative medicine.

## Introduction

Mechanotransduction enables cells to sense and adapt to forces and physical constraints imposed by the ECM (Vogel and Sheetz, 2006; Schwartz, 2010). The ECM supports morphogenetic processes during embryonic development or cancer and during tissue homeostasis in adulthood. Apart from providing a structural support, the chemical and physical properties of the ECM control tissue architecture by driving specific cell differentiation programs (Mammoto and Ingber, 2010). Soluble growth factors are chemical cues incorporated into the ECM. Their distribution, activation, and presentation to cells are spatially regulated by the physical properties of the ECM (Discher et al., 2009; Hynes, 2009; Tenney and Discher, 2009). However whether growth factors are able to initiate a mechanical response is still a matter of debate. Although it is known that cell mechanics control gene transcription for the maintenance of pluripotency, the determination of cell fate, pattern formation and organogenesis (McBeath et al., 2004; Gilbert et al., 2010; Lu et al., 2012), the signaling pathways regulating the activity of nuclear transcription factors in response to these physical signals are not well understood.

Bone morphogenetic proteins (BMPs) belong to the transforming growth factor β superfamily. They have been shown to participate in patterning and specification of several tissues and organs during vertebrate development. They regulate cell growth, apoptosis and differentiation in different cell types (Massagué, 2000; Capdevila and Izpisúa Belmonte, 2001). BMP-2, BMP-4, and BMP-7 are key molecules for normal bone development in vertebrates and induce osteoblastic differentiation of C2C12 mesenchymal pluripotent cells (Katagiri et al., 1994). Early events in BMP signaling are initiated through the phosphorylation of specific receptor-regulated Smad proteins, namely Smad1, Smad5, or Smad8. After phosphorylation, R-Smads form heteromeric complexes with the common mediator Smad4. These Smad complexes translocate to the nucleus and activate the transcription of specific target genes (Massagué and Wotton, 2000). Besides its role in bone differentiation, BMP-2 appears to control cytoskeletal rearrangements and cell migration, suggesting a role in mechanotransduction (Gamell et al., 2008; Kopf et al., 2014). However, little is known about the pathways involved in BMP-2–mediated cell adhesion and migration. Several studies have reported synergistic effects between integrin mechanoreceptors and growth

Correspondence to Corinne Albiges-Rizo: corinne.albiges-rizo@ujf-grenoble.fr; or Catherine Picart: catherine.picart@grenoble-inp.fr

Abbreviations used in this paper: ALP, alkaline phosphatase; bBMP-2, matrix-bound BMP-2; BMPR, BMP-2 receptor; CL, cross-linked; cRGD, cyclic RGD; FN, fibronectin; GM, growth medium; GSK, glycogen synthase kinase; ILK, integrin-linked kinase; LIMK, LIM kinase; PLL, poly(L-lysine); ROCK, rhoA-associated kinase; sBMP-2, soluble BMP-2; TCPS, plastic substrate.

© 2016 Fourel et al. This article is distributed under the terms of an Attribution–Noncommercial–Share Alike–No Mirror Sites license for the first six months after the publication date (see http://www.rupress.org/terms). After six months it is available under a Creative Commons License (Attribution–Noncommercial–Share Alike 3.0 Unported license, as described at http://creativecommons.org/licenses/by-nc-sa/3.0/).

The Rockefeller University Press $30.00
J. Cell Biol.
www.jcb.org/cgi/doi/10.1083/jcb.201508018



THE JOURNAL OF CELL BIOLOGY

Downloaded from jcb.rupress.org on March 7, 2016

Published March 7, 2016

factor signaling pathways (Comoglio et al., 2003; Margadant and Sonnenberg, 2010; Ivaska and Heino, 2011) without a particular focus on integrins and BMP receptor cooperation. Whether these BMP responses depend on the recruitment of integrin mechanoreceptors or on the cross-talk with additional pathways remains to be elucidated. It is still not known which receptor initiates signaling and whether such cross-talk involves (a) membrane-proximal interactions or (b) cooperation in the downstream signal transduction pathways. The difficulty comes from used experimental conditions that do not discriminate between growth factor presentation (usually diluted in culture medium) and ECM physical properties (imposed by the material on which cells are cultured).

We have shown that a biomimetic material can be used to present BMP-2 in a matrix-bound manner to control cell fate by inducing bone differentiation in vitro and in vivo (Crouzier et al., 2009, 2011a). We have also shown that matrix-bound BMP-2 affects cell spreading and cell migration (Crouzier et al., 2011a). Here, our goal was to understand how integrin and BMP-2 signaling are biochemically interpreted and connected through the BMP-2-induced Smad cascade. To gain insight into the possible cross-talk between BMP and adhesion receptors, we uncoupled ECM stiffness from biochemical signals transduced by BMP-2 using a biopolymeric biomaterial. We investigated how biochemical cues provided by matrix-bound BMP-2 may affect cell mechanical responses and drive a genetic program. We show that BMP-2 receptors and β3 integrins cooperate and coordinate a cellular response to control both cell spreading and Smad signaling. The spatial organization of BMP-2 presented in a "soft matrix–bound" manner is sufficient to trigger cell spreading and migration overriding the stiffness response through actin and adhesion site dynamics. In turn, αvβ3 integrin is required for BMP-2–induced Smad signaling by controlling both BMP-2 receptor (BMPR) activity and Smad stability. Our data show that BMP and integrin signaling converge to couple cell migration and fate commitment.

## Results

### Matrix-bound BMP-2–BMPR interaction alters the stiffness response of C2C12 cells

To mimic in vitro the likely context of BMP-2 presentation in vivo, we used a thin biomaterial made by self-assembly of hyaluronan (HA) and poly(L-lysine) (PLL). Adapting the cross-linker concentration to obtain either low cross-linked (CL) or high-CL films enabled us to modulate film stiffness (Table S1) as previously described (Boudou et al., 2011; Crouzier et al., 2011a). Hereafter, low-CL and high-CL films will be named soft and stiff conditions, respectively. BMP-2 is simply post-loaded on the film to obtain matrix-bound BMP-2 (bBMP-2) as the film presents high affinity toward BMP-2 (Crouzier et al., 2009). The amounts of loaded BMP-2 were similar for soft and stiff films with 740 ± 120 and 970 ± 180 ng/cm$^2$ of adsorbed BMP-2, respectively. These biomimetic films offer the advantage of presenting BMP-2 to cells in a matrix-bound manner and promote localized BMP-2 signaling. They are truly unique in their ability to present BMP-2 to cells in a matrix-bound manner, as BMP-2 is a very sensitive protein able to quickly lose its bioactivity and difficult to graft on surfaces in controlled amounts (King and Krebsbach, 2012). The films behave as nano-reservoirs for stable and bioactive BMP-2 molecules (Fig. S1 A). They can turn on the BMP-responsive element luciferase reporter gene (BRE-Luc; Fig. S1 B), phosphorylation of BMP-2-regulated transcription factors Smad at the C-terminus (pSmad1$^{Cter}$; Fig. S1 C), expression of alkaline phosphatase (ALP; Fig. S1 D) and they induce bone growth in vivo at ectopic site (Crouzier et al., 2011b).

C2C12 myoblasts represent a well-accepted in vitro model system to study the ability of BMP-2 to alter cell lineage from the myogenic to the osteogenic phenotype (Katagiri et al., 1997; Yamamoto et al., 1997). As expected, plastic substrate (TCPS) or films of different stiffness did not activate the Smad signaling pathway in the absence of BMP-2 (Fig. S1). Compared with delivery of soluble BMP-2 (sBMP-2), the presentation of matrix-bound BMP-2 (bBMP-2) potentiated the Smad response in cells on soft films whereas it did not improve the Smad response in cells grown on stiff films (Fig. S1). This reveals interference between substrate stiffness and BMP-2 signaling, stressing the necessity of working under conditions of high matrix compliance when attempting to elucidate BMP-2-mediated cell signaling.

We then compared C2C12 cell spreading at early times (4 h). This time point corresponds to an optimal spreading (threefold increase between 30 min and 4 h) and avoids the large variability in the kinetics of cell spreading on the polyelectrolyte films at earlier time points (Crouzier et al., 2011a). Of note, C2C12 cell spreading on low CL films with bBMP-2 can be maintained for at least 24 h (Fig. S2 A). As anticipated from our previous experiments (Ren et al., 2010) and from studies of natural and synthetic gels of various stiffness (Discher et al., 2005), the cells spread more on stiff films than on soft ones (Fig. 1 A). On stiff films, exposure to matrix-bound BMP-2 did not induce any changes in cell adhesion or spreading (Fig. 1 A). In contrast, whereas C2C12 myoblasts were round and poorly spread on soft films in the absence of BMP-2 or with exposure to sBMP-2, exposure to bBMP-2 induced a drastic increase in cell adhesion and spreading (Fig. 1 A). We examined whether cell spreading was initiated by BMP-2 receptors after sensing matrix-bound BMP-2. To do so, we investigated whether knockdown of BMPR-Ia and of BMPR-II, known to be expressed in C2C12 cells (Nohe et al., 2002), could impact C2C12 cell spreading induced by BMP-2 bound to soft films (Fig. 1 B). The efficiency of siRNA-mediated BMPR-Ia and BMPR-II silencing was determined by quantitative PCR analysis, which showed a specific decrease of targeted mRNA expression (Fig. 1 C). C2C12 cell spreading was strongly reduced in response to bBMP-2 on soft films after BMPR-Ia or BMPRII receptor depletion (Fig. 1 B).

Our results indicate that BMPR-Ia receptors and to a lesser extent BMPR-II receptors are involved in C2C12 myoblast spreading induced by soft matrix–bound BMP-2. The biomaterial provides BMP-2 confinement and promotes localized BMP-2 signaling that is sufficient to induce cell spreading independently of substrate stiffness. In other words, matrix-bound BMP-2 alters the stiffness response of C2C12 cells via interactions with BMPR.

### β3 integrin is required for cell spreading in response to matrix-bound BMP-2

As integrins play a key role in adhesion, spreading, and mechanotransduction (Albiges-Rizo et al., 2009), in particular in early adhesion of myoblasts and their subsequent fusion to form myotubes (Mayer, 2003), we investigated their

Downloaded from jcb.rupress.org on March 7, 2016

Published March 7, 2016

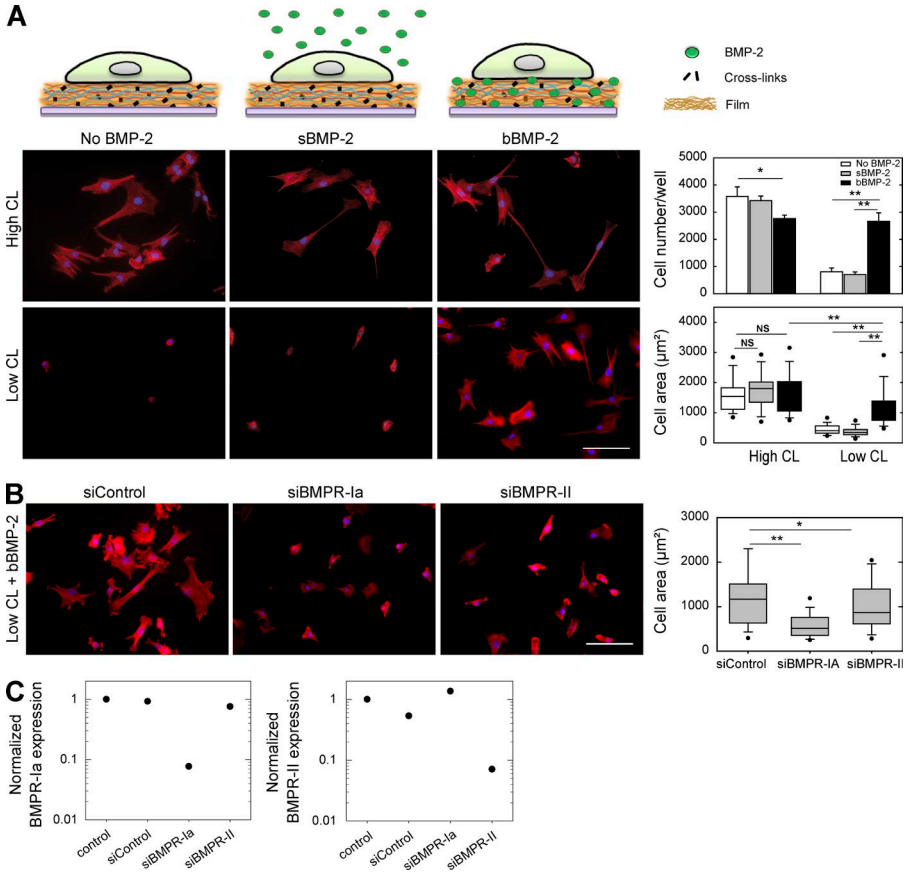



Figure 1. **Soft matrix–bound BMP-2 is sufficient to induce cell spreading.** (A, left) C2C12 cells morphology observations after 4 h of plating on the biopolymeric films with soluble BMP-2 (sBMP-2) or matrix-bound BMP-2 (bBMP-2). Actin and nucleus staining of C2C12 cells revealed well-spread morphology on high-CL films in the absence of BMP-2 or presence of sBMP-2 or bBMP-2. In contrast, for cells on low-CL films, bBMP-2 induced a striking increase of cell spreading as compared with sBMP-2. (A, right) Quantification of cell number and spreading shows the drastic increase in cell spreading in response to soft matrix–bound BMP-2. (B, left) C2C12 cells were depleted in BMPR-Ia or BMPR-II using siRNA. (B, right) After 4 h of plating, cell area on soft matrix-bound BMP-2 was quantified by visualizing cells F-actin. (C) Confirmation of efficiency of BMPR-Ia and BMPR-II deletion by quantitative PCR analysis. Bar, 100 µm. Data are means ± SEM 60 cells per condition are analyzed ($n$ = 3). NS, not significant; *, $P \leq 0.05$; **, $P \leq 0.005$.

possible involvement in cell spreading induced by BMP-2 ligand bound to the soft matrix. The appearance of focal adhesions, as assessed by vinculin staining, and the development of actin stress fibers were correlated with cell spreading on matrix-bound BMP-2 to soft films (Fig. 2 A). Moreover, manganese treatment was sufficient to induce cell spreading in the absence of BMP-2 (Fig. 2 B), suggesting that cell spreading might be the result of integrin activation, which was visualized by the increase in vinculin containing focal adhesions (Fig. 2 B). Of note, bBMP-2–induced cell spreading was also observed in the absence of serum (Fig. S3 A; Crouzier et al., 2011a), excluding the presence of a soluble mediator in the serum.

To gain further insight into the spatial organization of adhesion receptors in C2C12 cells spread on matrix-bound BMP-2 films, we labeled integrins using specific antibodies. Only very small clusters of integrins were visible at the surface of cells spread in the absence of matrix-bound BMP-2 (Fig. 2 C, top). Conversely, we observed that matrix-bound BMP-2 induced an increase in integrin receptor clustering and the organization of focal adhesions containing α5, αV, β1, and β3 integrins at the basal cell surface (Fig. 2 C, bottom). To confirm the role of β1 or β3 integrins, we investigated whether integrin-blocking antibodies (Fig. 2 D) or knockdown by RNAi (Fig. 2 E) could affect cell spreading induced by matrix-bound BMP-2 on soft films. The effect of siRNA-mediated silencing of β1 or β3 chains was efficient and identical, as judged by Western blot analysis (Fig. 2 F). Strikingly, blocking $\beta_3$ integrin greatly decreased the number of adherent and spread cells as compared with $\beta_1$ integrin blockade (Fig. 2 D). Using integrin-blocking antibodies against α chains revealed that $\alpha_V$ integrins were also implicated in the process of cell spreading, suggesting the involvement of $\alpha_v\beta_3$ integrins in BMP-2 mediated cell spreading (Fig. S2 B).

Our results show that matrix-bound BMP-2 induces αvβ3 integrin clustering. We next determined whether β3 integrin is engaged with a ligand in these BMP-2–induced focal adhesions. To do so, we set up a competition assay using cyclic RGD (cRGD), a specific ligand for β3 integrin (Dechantsreiter et al., 1999), to compete with potential endogenous ligands. We showed that cRGD inhibited cell spreading onto BMP-2–soft matrix in contrast to the negative control cRAD (Fig. S2 C), confirming that β3 integrin is engaged with its ligand in BMP-2–induced focal adhesions. The notion that β3 integrins are involved in cell spreading induced by matrix-bound BMP-2 on soft matrix can be extended to other cell types, as we found that mouse mesenchymal stem cells (D1MSC) respond to bBMP-2 and that this response is impaired by cRGD treatment (Fig. S2 D). Together, these results demonstrate that β3 integrin needs to be occupied by its ligand to drive cell spreading onto BMP2–soft matrix in cell lines able to respond to bBMP-2. The subsequent question addressed the identity of the ligand of β3 integrin. Fibronectin (FN), which is one of the β3 integrin ligands, effectively decorated cell edges, as observed by immunostaining of C2C12 cells plated on low-CL films with or without of bBMP-2 (Fig. S3). FN could be provided either by the cells or by the serum. The role of serum can be ruled out, because cell spreading is still possible onto matrix-bound BMP-2 in the absence of serum (Fig. S3 A; Crouzier et al., 2011a). Moreover, the presence of FN around the cells was independent of the presence of serum in the culture medium (Fig. S3 A). Cells expressed FN as measured by quantitative PCR, and this expression was not affected by BMP-2 treatment after 4 h of adhesion (Fig. S3 B). An increase in the FN and collagen mRNA

Downloaded from jcb.rupress.org on March 7, 2016

Published March 7, 2016

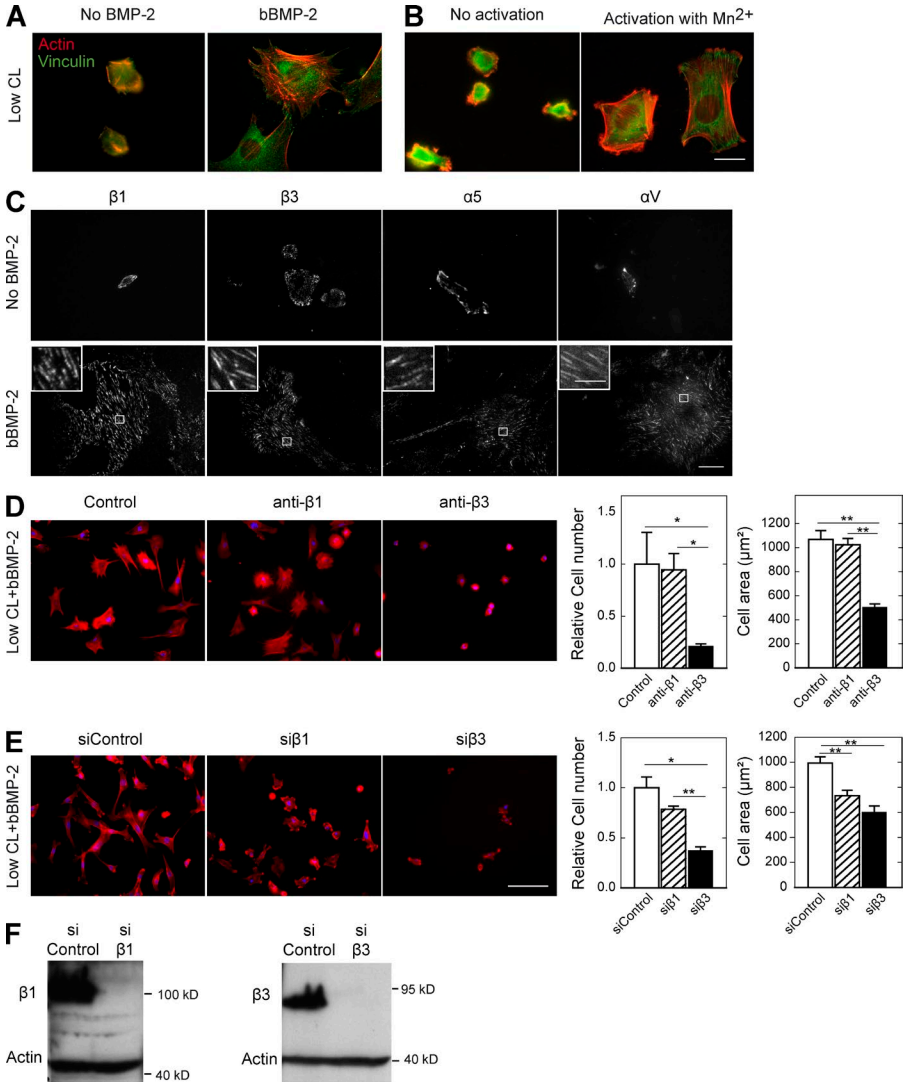



Figure 2. **β3 integrin is required for cell spreading induced by bBMP-2 on soft films.** (A) C2C12 myoblasts plated for 4 h on soft films without BMP-2 (left) or with bBMP-2 (right) were stained for actin and vinculin, indicating the presence of focal adhesions in the case of bBMP-2. (B) C2C12 myoblasts plated for 4 h on soft films without or with $Mn^{2+}$ stimulation were stained for actin and for vinculin. (C) Cells 4 h after seeding on soft films without BMP-2 or with bBMP-2 were stained for $\beta_1$, $\beta_3$, $\alpha_5$, and $\alpha_V$ integrin subunits. Insets show zoom-in of the focal adhesions. (D) C2C12 cells were incubated in the absence or presence of β1 and β3 integrin blocking antibodies (D, left) or depleted in $\beta_1$ and $\beta_3$ integrin chains using siRNA strategy before plating on soft films with bBMP-2 (E, left). (D and E, right) After 4 h, adherent cell number and spreading area quantified by actin staining significantly decreased in the presence of anti-$\beta_3$ integrin or after treatment with siRNA against β3 integrin on soft film with bBMP-2. Data are means ± SEM from at least 60 cells per condition. Experiments were performed three times. (F) Western blot analysis confirms the efficiency of the siRNA against integrins. *, $P \leq 0.05$; **, $P \leq 0.005$. Bars: (A and C) 20 µm; (insets) 5 µm; (D and E) 100 µm.

levels became significant only after 30 h of culture (Fig. S3 B). To test whether β3 integrin binds to this FN to induce a cell response, C2C12 cells were treated with siRNA against FN. Depletion of FN abolished cell spreading onto BMP-2–soft matrix (Fig. S3 C). These results indicate that αvβ3 integrin binds to FN surrounding C2C12 cells to promote BMP-2–induced cell spreading.

Knowing that BMP-2 is able to bind FN through its FN 12–14 domains (Martino et al., 2011, 2014), we tested whether FN might bind matrix-bound BMP-2 on soft matrix. Using fluorescence spectroscopy, we showed that a much higher amount of FN can adsorb to the soft films loaded with matrix-bound BMP-2 in comparison to films without BMP-2 (Fig. S3 D). Of note, although hyaluronan might be involved in cells adhering onto the polyelectrolyte films, our previous data on low- and high-CL films using either soluble hyaluronan in solution or HA blocking antibodies did not allow us to reveal a specific effect of hyaluronan (Ren et al., 2010).

Our data indicate that, in addition to the transcriptional response, matrix-bound BMP-2 is sufficient and necessary to induce an early mechanical response, e.g., C2C12 or mouse mesenchymal stem cell spreading, likely through αvβ3 integrin activation. In summary, BMP-2 loaded onto the film is able to provide two anchoring points for cell spreading: one through BMP-2–BMPR interaction for initiating cell spreading and the second through BMP-2–FN–αvβ3 integrin for completing the spreading. These findings support the notion of cooperation between BMP-2 receptors and β3 integrins on soft films containing matrix-bound BMP-2.

## Matrix-bound BMP-2 increases cell migration by affecting cell adhesion site dynamics

As integrins and BMP-2 in a soluble form have been shown to be involved in cell migration (Dudas et al., 2004; Goldstein et al., 2005; Huttenlocher and Horwitz, 2011; Plotnikov and Waterman, 2013), and as we previously showed that bBMP-2 is involved in cell migration (Crouzier et al., 2011a), we analyzed whether BMP-2 presentation would affect the migration behavior of C2C12 cells by altering adhesion site dynamics. Two approaches were used, including time-lapse imaging and FRAP analysis of focal adhesions. Cell tracking assays over 15 h confirmed the ability of bBMP-2 to increase cell migration in soft and stiff conditions (velocity of 42 and 38 µm/h, respectively), whereas sBMP-2 did not significantly increase cell migration in both conditions (velocity of 7 and 17 µm/h, respectively) as compared with conditions without BMP-2 (velocity of 6 and 19 µm/h, respectively; Fig. 3 A). Moreover, β3 integrin was shown to be involved, as migration speed was decreased by twofold in

Downloaded from jcb.rupress.org on March 7, 2016

Published March 7, 2016

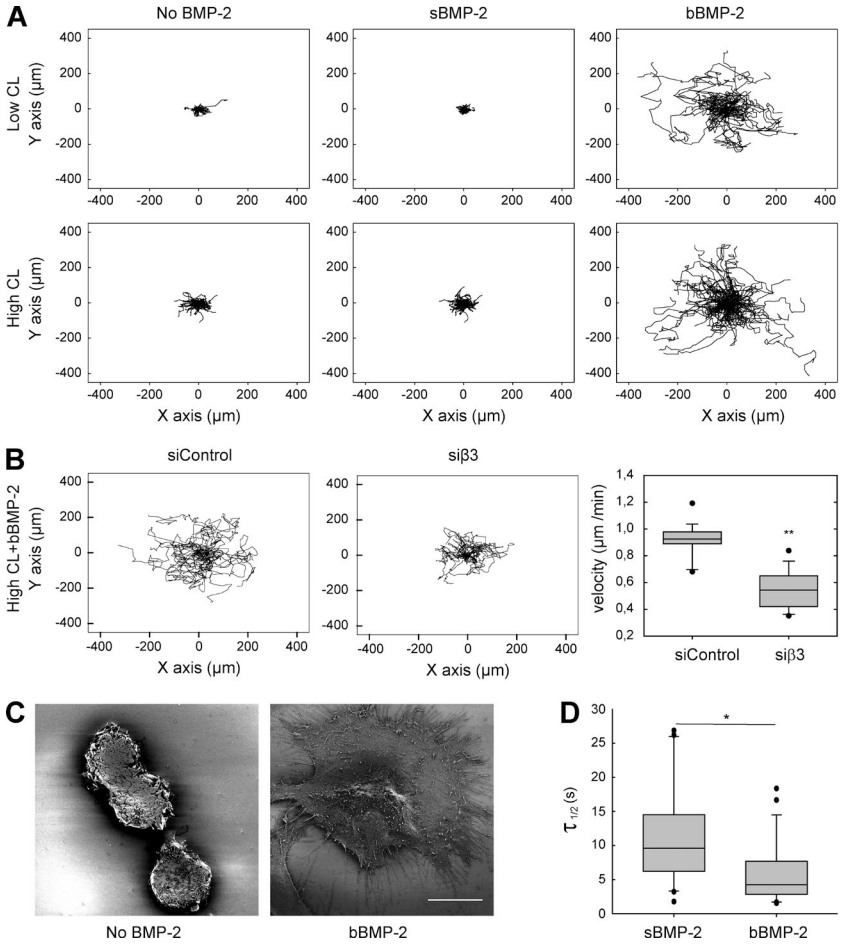



Figure 3. **Matrix-bound BMP-2 increases cell migration by affecting focal adhesion dynamics.** (A) Tracking experiments of C2C12 cells plated on low- or high-CL films without BMP-2 or treated with sBMP-2 or bBMP-2. The plotted trajectories of 15 h time-lapse experiments highlight the increased migration speed of cells plated on bBMP-2 whatever the film stiffness. 60 cells per condition are analyzed. (B) C2C12 cells plated on high-CL films with bBMP-2 have been monitored in conditions where β3 integrin was depleted as compared with siControl. As quantified, the deletion of β3 integrin abolished this increase of cell migration. 60 cells per condition are analyzed. (C) Scanning electron microscopy images of C2C12 cells plated on soft film without BMP-2 or treated with bBMP-2. Note the increase of filopodia when cells are subjected to matrix-bound BMP-2. Bar, 10 µm. (D) Quantitative measurement of the characteristic recovery time (τ) measured on individual focal adhesion using GFP-paxillin ($n$ = 20). The shorter recovery time indicates a higher mobility of GFP-paxillin in the case of C2C12 cells spread onto bBMP-2 in comparison to sBMP-2. *, $P \leq 0.05$; **, $P \leq 0.005$.

case of β3 integrin deletion (Fig. 3 B). These results show that the presentation of BMP-2 by the matrix has a crucial influence on cell migration. Morphological analysis by scanning electron microscopy revealed a marked generation of filopodia in cells on bBMP-2 (Fig. 3 C), suggesting a role of BMP-2 in organization of the actin cytoskeleton. We next investigated the possible effects of BMP-2 presentation on focal adhesion dynamics by quantifying the exchange rate of focal adhesion components (Fig. 3 D) after C2C12 cell transfection of with GFP-paxillin to study single focal adhesions. Cells were plated on stiff films in the presence of sBMP-2 or bBMP-2 to enable cell spreading independently of BMP-2 presentation. Our results revealed that the GFP-paxillin recruitment to focal adhesions was twofold slower in the case of sBMP-2 as compared with bBMP-2. First, our findings show that matrix-bound BMP-2–induced cell migration is not modulated by substrate stiffness. Second, our results suggest that the presentation of BMP-2 by the matrix impacts the dynamics of focal adhesions through a faster recruitment of focal adhesion components such as paxillin.

### αvβ3 integrin is required to mediate BMP-2–induced Smad signaling pathway through a Src-FAK- ILK-cdc42 axis

As a counterpart to BMP-2 involvement in focal adhesion dynamics, we next investigated whether β3 integrins are in turn required in a cross-talk for BMP-2–induced Smad signaling. To explore the roles of BMP receptors and integrins in Smad signaling by matrix-bound BMP-2, we examined the Smad response using a luciferase reporter assay and Smad phosphorylation (pSmad1,5, $8^{Cter}$; Fig. 4). As the luciferase signal is increasing as a function of time by displaying a threefold higher signal at 8 h and a sixfold higher signal at 24 h than at 4 h, the time point of 15 h was selected for luciferase analysis to be able to quantify the effect of drugs or siRNA (Fig. 4 C). As expected, knockdown of BMPR-Ia and of BMPR-II receptors had a strong negative effect on both BMP-2-induced reporter activities and Smad phosphorylation. Strikingly, depletion of β3 integrins led to a two- and threefold decrease in Smad1 phosphorylation at its C terminus (Fig. 4, A and B) and in the activity of ID1 promoter in a BMP-responsive element luciferase reporter gene assay (BRE-Luc), respectively (Fig. 4 D), which was not the case for β1 integrin deletion. The results obtained in the case of β3 knockdown were similar to those obtained after knockdown of BMP receptors (Fig. 4, A, B, and D). As a control, we used dorsomorphin, an inhibitor of BMP signaling (Yu et al., 2008) known to selectively inhibit BMP type I receptors ActR-I, BMPR-Ia and BMPR-Ib by preventing phosphorylation of Smad proteins (Fig. 4 D). Whereas dorsomorphin treatment inhibited Smad phosphorylation as well as luciferase activity, it did not impair cell spreading (Fig. 5 B). Thus, our data show that β3 integrin is required to mediate BMP-2–induced Smad signaling. In addition, our results demonstrate that the phosphorylation of Smad is not involved in β3 integrin–dependent spreading which is induced by BMP-2. Altogether these results suggest that the spreading is rather caused by the BMP-2/BMPR interaction upstream of Smad phosphorylation, identifying β3 integrin activation as an early event after BMP-2 binding to BMPR. Moreover, the cooperation between BMP receptors and β3 integrins is required for effective Smad signaling in myoblasts in response to matrix-bound BMP-2.

Downloaded from jcb.rupress.org on March 7, 2016

Published March 7, 2016

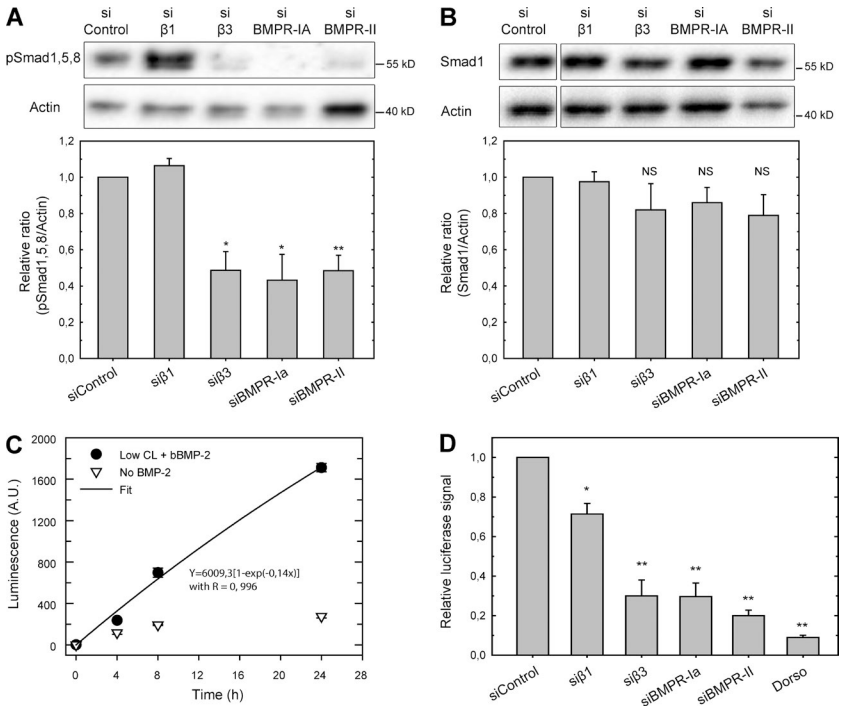



Figure 4. **β3 integrins are required to mediate Smad signaling.** C2C12 cells were transfected with siRNA against β chain integrins, BMPR-Ia, or BMPR-II and plated on soft matrix with bBMP-2 for 4 h. Western blot and quantification of phospho-Smad1,5,8 (A) and Smad1 (B). Smad pathway activation significantly decreased when cells were transfected with siRNA against β3 integrin, BMPR-Ia, or BMPR-II. (C) Kinetics of luciferase signal in C2C12 cells plated on soft matrix with or without bBMP-2. (D) Analysis of luciferase activity upon dorsomophin (Dorso) treatment or upon deletion of BMP receptors and integrin receptors after 15 h of culture on soft film with bBMP-2. Data are mean ± SEM ($n$ = 3); NS, not significant; *, $P \leq 0.05$; **, $P \leq 0.005$, compared with siRNA control. A.U., arbitrary units.

Several transmembrane growth factor receptors, including PDGF and EGF receptors, are known to form multiprotein complexes with integrin receptors through Src and focal adhesion kinase (FAK), two cytoplasmic kinases associated with cell motility and spreading (Tomar and Schlaepfer, 2010), the adapter integrin-linked kinase (ILK; Brakebusch and Fässler, 2003), and RhoGTPase family activity (Tomar and Schlaepfer, 2009), reinforcing the link between actin cytoskeleton and integrin growth factor receptor complexes (Serrels et al., 2007). Therefore, the involvement of the FAK–Src signaling complex in the β3 integrin/BMP-2 receptor cooperation was explored using a pharmacological approach (Fig. 5). Inhibition of Src by PP2 and inhibitor number 5, nb5, of FAK by PF228 and of ILK by Cpd22 all decreased Smad activity in a dose-dependent manner (Fig. S4 A), as measured by the luciferase reporter assay (Fig. 5 A) and by Smad phosphorylation (Fig. 5 C). These results were confirmed using specific siRNA knockdown against Src, FAK, and ILK (Fig. 5 D). Actin filament organization is controlled by the Rho family of small GTPases, including Rho, Rac, and Cdc42 (Raftopoulou and Hall, 2004), partly regulated by PI3Kinase (Hanna and El-Sibai, 2013). To explore the mechanical events downstream of BMP-2 stimulation, we evaluated whether perturbations in small GTPase activities or cytoskeleton integrity could affect the Smad response (Fig. 5, A and C). PI3 kinase inhibition by LY294002 led to a decrease of luciferase activity (Fig. 5 A). Cdc42 inhibition by secramine (Pelish et al., 2006) or siRNA induced a decrease in Smad activity. In contrast, the Rho inhibitor Toxin C3 and the Rac inhibitor NSC23766 led to increased Smad signaling (Fig. 5, A, C, and D). To gain more insight into the potential role of the cytoskeleton in bBMP-2-induced Smad signaling on soft films, we used pharmacological agents known to interfere with cell tension or actin dynamics (Fig. 5, A and C). As indicated in Fig. 5 (A and C), treatment with the rhoA-associated kinase (ROCK) inhibitor (Y27632) or blebbistatin (blebb), which relieves tension on the actin cytoskeleton by inhibiting myosin-II, did not decrease Smad signaling. Interestingly, alteration of actin dynamics with cytochalasin D, an inhibitor that disrupts the actin cytoskeleton by capping filament plus ends, or latrunculin, which disrupts the actin cytoskeleton by preventing actin polymerization, reduced luciferase activity by 35% (Fig. 5 A). More importantly, inhibition of LIM kinase (ROCK and Cdc42 effector) by Pyr1 (Prudent et al., 2012), which is important for actin microfilament dynamics, showed a dose-dependent decrease of Smad activity down to 60% (Fig. 5 C and Fig. S4). As bBMP-2 induced spreading, we wondered whether cell shape could regulate Smad signaling. Our data show that the loss of Smad activation induced by Cdc42 inhibition, Src, and ILK is correlated with a decrease of cell spreading (Fig. 5, A and B). Only FAK inhibition did not follow this trend. In contrast, the absence of Smad phosphorylation by BMPR induced by dorsomorphin treatment had no effect on β3 integrin–mediated spreading (Fig. 5 B). We monitored the step after Smad phosphorylation, which is its nuclear translocation. Smad was already in the nucleus after 4 h of spreading onto bBMP-2 on soft matrix (Fig. S4, B and C). As a control, we showed that inhibition of Smad signaling using dorsomorphin was associated with a loss of nuclear localization. Consistently with our luciferase assays results, the nuclear localization of pSmad was decreased by ∼30–40% upon Src, FAK, or LIM kinase (LIMK) inhibition, whereas it was not affected by ROCK inhibition. As ROCK inhibition did not affect Smad phosphorylation, ROCK-dependent tension is not directly required for Smad activity in this β3 integrin/BMPR cross-talk. Our results suggest that instead, LIMK-dependent actin dynamics contribute to Smad signaling induced by bBMP-2 on soft matrix.

### β3 integrin regulates Smad stability by repressing GSK3 activity

After phosphorylation of Smad at the C terminus by BMPR, the duration of the pSmad1$^{Cter}$ signal is controlled by sequential phosphorylations of the Smad1 linker domain at consensus sites for MAPK and glycogen synthase kinase 3 (GSK3), which

Downloaded from jcb.rupress.org on March 7, 2016

Published March 7, 2016

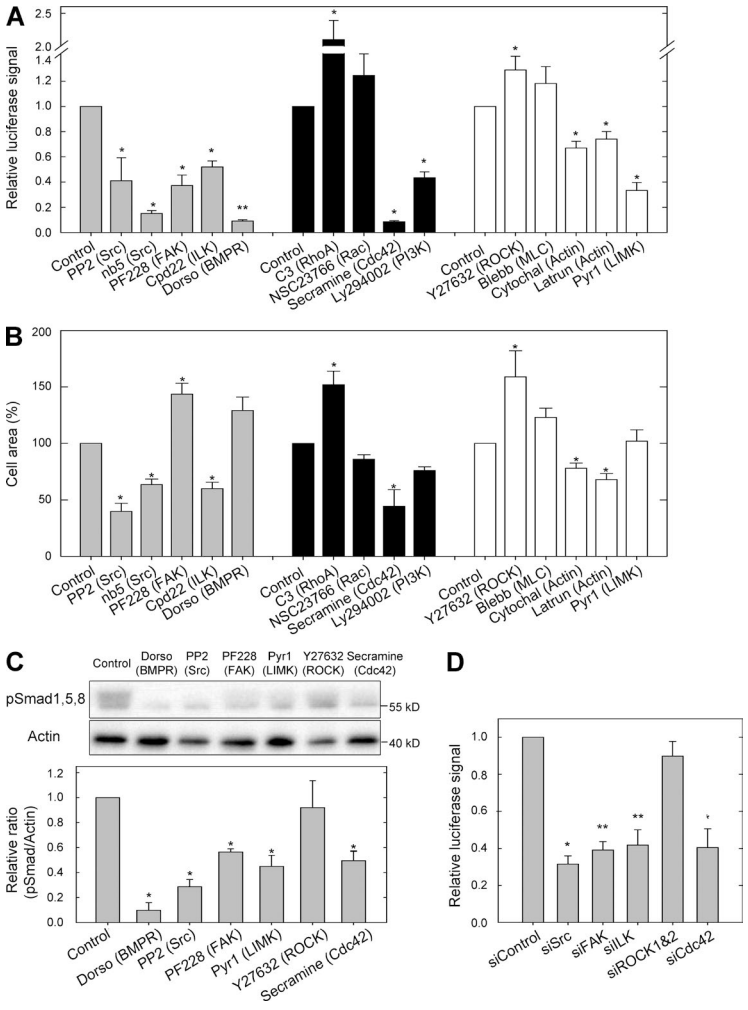



Figure 5. **Src, FAK, ILK, and Cdc42, but not ROCK, mediated BMP-2 signaling induced by bBMP-2.** (A) Luciferase activity of p(BRE) luciferase-transfected C2C12 cells was measured after 15 h of plating on soft film with bBMP-2 in the presence of various inhibitors of integrin and of Smad signaling (see list in Table S2). Gray panel: inhibitors of Src, FAK, ILK, and BMPR receptors PP2 (Src), nb5 (Src), PF228 (FAK), ILK (Cpd22), and dorsomorphin (BMPR); black panel: inhibitors of RhoGTPases C3 transferase (RhoA), NSC23766 (Rac), Secramine (Cdc42), Ly294002 (PI3 kinase); white panel: inhibitors of cell cytoskeleton and cell tension Y27632 (ROCK), blebbistatin (myosin II), cytochalasin D, latrunculin (F-actin), and Pyr1 (LIMK). (B) Cell spreading area of C2C12 cells cultured for 4 h on soft films with bBMP-2 in the presence of the same inhibitors as for A was quantified. For cell spreading analyses, 60 cells were analyzed per condition ($n$ = 3). Data are mean ± SEM. The control condition (bBMP-2 on soft films) was normalized to 1 or 100% for luciferase signal and cell spreading, respectively. (C) Effect of inhibitors on Smad1,5,8 phosphorylation. Western blot of phospho-Smad1,5,8 (C, top) and corresponding quantitative analysis (bottom) after cell culture for 4 h on soft films with bBMP-2 in the presence of various inhibitors: dorsomorphin (BMPR), PP2 (Src), PF228 (FAK), Pyr1 (LIMK), Y27632 (ROCK), and Secramine (Cdc42). (D) Measurement of luciferase activity after 15 h of culture on soft film with matrix-bound BMP-2 upon siRNA treatment against Src, FAK, ILK, ROCK1&2, and Cdc42. The control condition (bBMP-2 on soft films) was normalized to 1 for luciferase signal. Data are mean ± SEM ($n$ = 3); *, $P \leq 0.05$; **, $P \leq 0.005$, compared with the control condition.

are required for Smad1 proteasomal degradation (Fuentealba et al., 2007; Aragón et al., 2011). GSK3 is negatively regulated by ILK, a downstream effector of β3 integrins (Delcommenne et al., 1998). As we have previously shown a decrease of pSmad1$^{Cter}$ (Fig. 4 A) upon depletion of β3 integrin, we addressed the question whether β3 integrin regulates the stability of pSmad1$^{Cter}$ by controlling Smad1 phosphorylation by GSK3 downstream of ILK. First, we showed that after spreading onto matrix-bound BMP-2 on soft matrix, the depletion of β3 integrin, as opposed to β1 integrin depletion, totally abolished the phosphorylation of GSK3, demonstrating that GSK3 activity is regulated by β3 integrin (Fig. 6 A). Consistently, we found that after treatment with cycloheximide, an inhibitor of protein synthesis, the duration of Smad signaling was decreased after β3 integrin depletion (−50% after 3 h) in comparison to control conditions (−50% after 6 h; Fig. 6 C), indicating that β3 integrin-dependent phosphorylation of GSK3 leads to Smad degradation. Downstream of β3 integrin, ILK was also necessary to repress GSK3 activity, as judged by the loss of GSK3 phosphorylation upon ILK deletion (Fig. 6 A). Strikingly, treatment with a GSK3 inhibitor (SB216763) was able to rescue luciferase reporter activity after depletion of the downstream effectors of β3 integrins, especially ILK, Src, or FAK, pinpointing GSK3 as their downstream target (Fig. 6 B). However, GSK3 inhibitor treatment was not efficient in rescuing the luciferase signal after deletion of β3 integrin (Fig. 6 B), emphasizing an upstream priming role of β3 integrin in the activation of BMPR. We also noticed that the deletion of BMPR-Ia was more efficient than the deletion of BMPRII in decreasing GSK3 phosphorylation, suggesting an important role of BMPR-Ia in the control of GSK3 by β3 integrin (Fig. 6 A).

Our results were extended to mesenchymal stem cells (D1MSC) where the phosphorylation of Smad and GSK3 was also inhibited after β3 deletion (Fig. S5 C). Importantly, phosphorylation of GSK3 is not dependent on cell spreading but associated with β3 integrin signaling. Indeed, in conditions where C2C12 cell spreading was imposed by the presence of a stiff substrate (tissue culture polystyrene), cell spreading was not affected by the deletion of β3 integrin (Fig. S5 A) but was still associated with a decrease of both Smad (−30%) and GSK3 (−50%) phosphorylations (Fig. S5 B).

Our results demonstrate that β3 integrin regulates a multistep process to control Smad activity. First, β3 integrin is important for assisting BMPR to phosphorylate Smad1 at its C terminus independently of GSK3 activity. Second, β3 integrin is crucial for the stability of pSmad1$^{Cter}$ by repressing the activity of GSK3 through the downstream Src–FAK–ILK axis.

## Discussion

In this study, matrix-bound BMP-2 allowed us to dissociate physical and biochemical cues to understand how cells integrate multiple signaling pathways to couple cell migration and cell

Downloaded from jcb.rupress.org on March 7, 2016

Published March 7, 2016

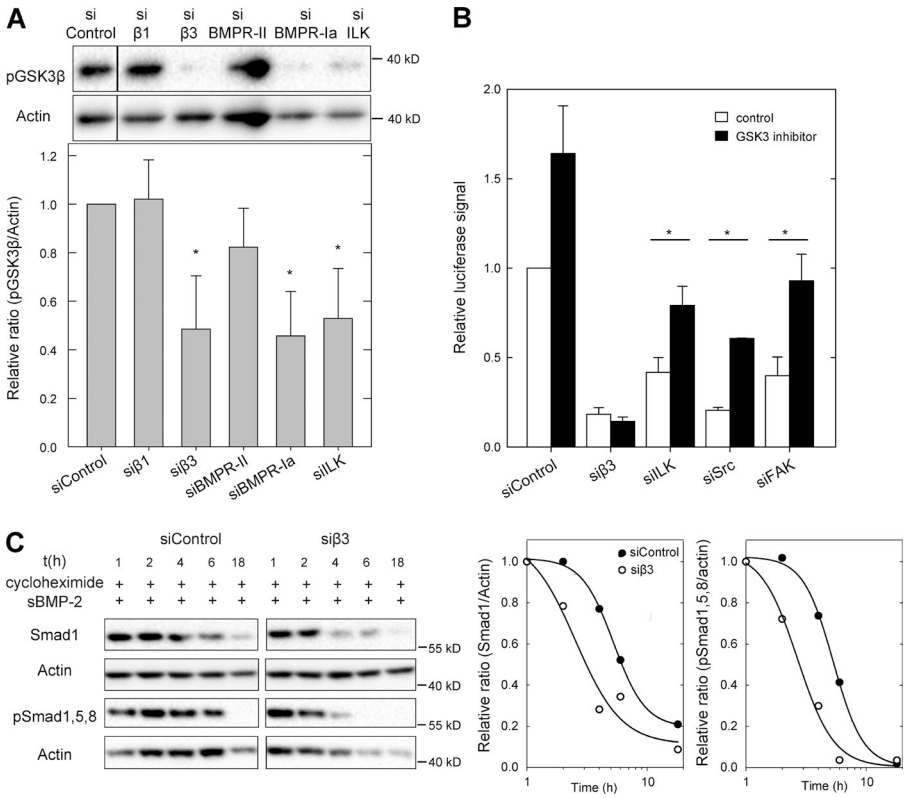



Figure 6. **β3 integrin influences BMP-2 signaling through GSK3β inhibition.** (A, top) After depletion of β1 integrin, β3 integrin, BMPR-II, BMPR-Ia, and ILK, C2C12 cells are spread onto matrix-bound-BMP-2 for 4 h and the level of GSK3β activity is determined by Western blot analysis by using anti–phospho-GSK3β antibody. (A, bottom) Quantification of GSK3β phosphorylation in the different conditions. Data are mean ± SEM ($n$ = 3). (B) Measurement of luciferase activity at 15 h upon siRNA treatment against β3 integrin, ILK, Src, and FAK with or without GSK3 inhibitor on soft film with bBMP-2. Data are mean ± SEM ($n$ = 3). (C) Monitoring of the life time of Smad1 and phospho-Smad1,5,8 in C2C12 cells spread on TCPS with sBMP-2. C2C12 cells depleted or not with β3 integrin were incubated with 100 µg/ml cycloheximide. Cycloheximide and sBMP-2 were added at $t$ = 0. Phospho-Smad1,5,8 and Smad1 protein contents in total lysates were visualized as a function of time from 1 to 18 h by Western blotting. The results are representative of three independent experiments. *, $P \leq 0.05$ compared with siRNA control.

differentiation. First, we demonstrate that matrix-bound BMP-2 is able to initiate a β3 integrin–dependent mechanical response in a BMPR-dependent and a Smad phosphorylation–independent manner. Second, we identify and give molecular insights into cooperation between β3 integrin and BMPR for controlling Smad signaling induced by matrix-bound BMP-2. We propose a model wherein β3 integrin is a key element that acts in a multistep process by controlling both the primary phosphorylation of Smad1 at its C terminus by BMPR and the stability of pSmad1$^{Cter}$ through the repression of GSK3 activity (Fig. 7).

Like many pluripotent mesenchymal cells, C2C12 myoblasts differentiate into distinct lineages depending on the nature of local cues and how they are presented in their environment. BMP-2 switches C2C12 cell lineage from the myogenic to the osteogenic phenotype (Katagiri et al., 1994). This osteoblastic lineage commitment in myoblasts is associated with a microenvironmental change that occurs over several days (Ozeki et al., 2007). Our study aimed to decipher the initial steps of BMP-2 response in the osteogenic induction and the involvement of β3 integrin in Smad signaling.

First, we have shown that matrix-bound BMP-2 through its interaction with BMPR is sufficient to induce the initiation of an adhesive and promigratory phenotype through β3 integrin clustering, reorganization of the cytoskeleton through stress fibers, filopodia formation, and an increase in adhesion site dynamics. Our results are in line with previous observations showing the involvement of BMP family in cell migration (Sieber et al., 2009). We have shown that the β3 integrin–dependent cell spreading is favored by the natural interactions existing between BMP-2 and FN produced by the cells (Martino et al., 2011, 2014). In addition to its interaction with BMPR, BMP-2 bound to the biomaterial is able to interact with FN secreted by C2C12 cells. Consequently, the biomaterial presenting BMP-2 is able to provide two anchorage points for cells: BMP-2–BMPR interaction initiates the formation of focal adhesions containing FN-engaged β3 integrin and BMP-2–FN interaction supports anchorage of β3 integrin to the biomaterial. The topology of this biomaterial has been essential to optimize the proximity between β3 integrin and BMPR, hence favoring their cross-talk.

Additionally, we have shown that the role of β3 integrin upon BMP-2 stimulation is not restricted to cell migration and spreading but is crucial for the initiation of Smad signaling via a multistep process. The activation of β3 integrin is the first event of the β3 integrin–BMPR cross-talk. It requires neither the phosphorylation of Smad at C terminus nor the tyrosine kinase activity of BMPR. Indeed, dorsomorphin treatment upon BMP-2 stimulation inhibits BMPR activity but still preserves β3 integrin–mediated cell spreading. We have also demonstrated that, in turn, β3 integrin is necessary for early events in BMP-2 signaling to allow the primary C-terminal phosphorylation of Smad by BMP receptors. The inability of a GSK3 inhibitor to rescue luciferase activity in conditions where β3 integrin is deleted indicates that the activation of BMPR by β3 integrin is upstream to the inhibition of GSK3 by β3 integrin. The use of a biomaterial presenting BMP-2 in a matrix-bound manner has been critical to unveil the involvement of β3 integrin in the initiation of Smad signaling. Because soft matrix does not sustain high numbers of cell attachment for long periods of time, future experiments will need to test whether this limitation can be rescued with substrate-bound ligands such as anti–BMPR-Ia. Our study underlines the importance of growth factor presentation such as BMP-2 in a soft context to properly elucidate the molecular mechanisms underlying the perception of biochemical and physical cues of the microenvironment as already described for VEGF (Chen et al., 2010) and EGF (Fan et al., 2007).

Finally, the cooperation between β3 integrin–GSK3 and the BMP-2–Smad pathway highlights the coupling between cell migration and cell-fate commitment. It has been previously

Downloaded from jcb.rupress.org on March 7, 2016

Published March 7, 2016

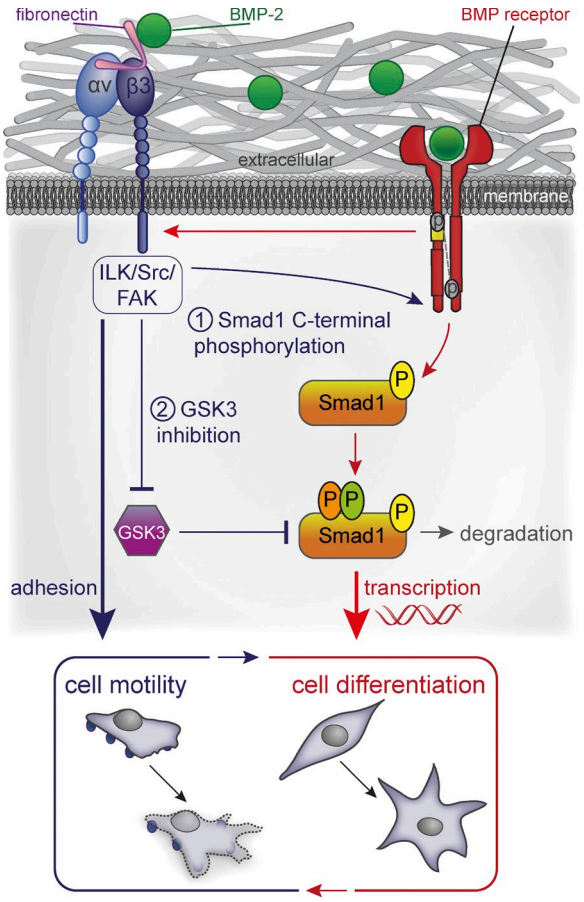



Figure 7. **Schematic view of β3 integrin–GSK3β and BMP-2–Smad cooperation.** The interaction between BMP-2 and BMP-2 receptors activates αvβ3 integrin and mediate cell spreading and cell migration thanks to BMP2–FN interaction. In turn, αvβ3 is required first to allow the C-terminal phosphorylation of Smad by BMPR and second to inhibit GSK3 activity through the Src–FAK–ILK pathway. BMP receptors and β3 integrin signaling converge to control both focal adhesion dynamics and Smad signaling to couple cell migration and fate commitment.

shown that GSK3 phosphorylation regulates the duration of Smad signaling (Fuentealba et al., 2007; Sapkota et al., 2007). We demonstrate that GSK3 needs to be negatively controlled upstream by β3 integrin to modulate Smad phosphorylation and the Smad-associated transcriptional response, which are both important for the osteogenic switch. Consistently, it has been shown that pharmacological inhibition of GSK3 increases the osteogenic propensity of hMSCs cells (Krause et al., 2010). β3 integrin is not the only receptor that can regulate GSK3, because it has been already described that Wnt, PDGF, and FGF signaling can also modulate the GSK3 pathway (Biver et al., 2014; Song et al., 2014). Different cell surface receptors such as N-cadherin (Cheng et al., 1998) or the FGF receptor (Sailer et al., 2005) are also able to modulate BMP-2 responses. This suggests that mechanotransduction-dependent cell commitment results from receptor cooperation to specify the cellular response. It is also likely that both the biochemical and physical properties of the ECM in distinct tissues might dictate the molecular nature of the cluster or the cooperation.

BMP-2 stimulation and osteoblastic lineage commitment in myoblasts are associated with a microenvironmental change that occurs over several days, suggesting temporal and contextual effects (Ozeki et al., 2007). In our study, we focused our attention on short-term effects (4- to 15-h time window) mediated by BMP-2 before osteoblastic switch of C2C12 myoblasts observable after 1 d of BMP-2 stimulation. In light of an elegant series of micropattern experiments showing a relationship between cell shape and cell differentiation (McBeath et al., 2004), we suspected that cell shape and spreading imposed by β3 integrin activation might act as an early cue in the commitment process and be responsible for Smad signaling downstream of BMP-2 stimulation. Our data confirm that the spreading mediated by β3 signaling is induced by BMP-2 stimulation to initiate the Smad response. Whereas the shape-mediated control of osteoblastic lineage specification has been shown to involve cell tension and RhoA/ROCK signaling (Wang et al., 2012), our data demonstrate that the pathway activated by matrix-bound BMP-2 in myoblast cells leading to early Smad driven-transcription is dependent on Cdc42/LIMK and independent of Rho/ROCK activation. Although 4–8 h might not be sufficient time for significantly elevated transcription versus control (Fig. 4 C), the luciferase construct might not have the same kinetics as SMAD targets in the genome, although noncanonical pathways remain an alternative. This discrepancy may be explained by the timescale difference in BMP-2 stimulation and/or by differences in BMP-2 presentation: short term for BMP-2 presented from the soft matrix (4–15 h) in the present study as compared with longer term BMP-2 stimulation (2 d) for cells plated on a stiff micropatterned substrate with sBMP-2 (Wang et al., 2012). BMPR–β3 integrin cross-talk is likely to be relevant for the establishment of a transient new phenotype before the conversion from myoblasts to osteoblasts. Our results suggest that this conversion starts with Cdc42–LIMK pathway activation under the control of a cross-talk between β3 integrin and BMP receptors. However our observations derived from a soft matrix-bound BMP-2 are in line with the suppression of RhoA activity in compliant settings (Engler et al., 2006) and the ability of LIMK not only to interact with BMPRII (Foletta et al., 2003) but also to be activated via Cdc42–FAK pathway independently of ROCK pathway in myoblast cells (Gamell et al., 2008). Like physical cues (Engler et al., 2006; Swift et al., 2013; Dingal et al., 2015), our data show that BMP-2 as a biochemical cue is able to induce cytoskeletal reorganization that precedes the osteogenic switch. The involvement of β3 integrin and LIMK in the control of the phosphorylation of cofilin might support the need for temporal control of actin turnover, the necessity of continuous repression of actin depolymerization, or its participation in the formation of actin–cofilin rods important to initiate or support the osteogenic program (Dopie et al., 2012; Munsie et al., 2012; Sen et al., 2015). Our results do not exclude the involvement of the ROCK pathway and its control by another integrin at later stages of myoblast–osteoblast differentiation switch. Our results lead to the intriguing but intuitive idea that different integrins might have somewhat opposing or rather complementary mechanical roles during the time window of muscle-osteogenic trans-differentiation. Given the increase of ECM stiffness in osteoblastic lineage, which can be mimicked by a plastic substrate (McBeath et al., 2004), β1 integrin–ROCK signaling might substitute for β3 integrin–LIMK signaling later on during ECM stiffening upon the myoblast–osteoblast switch imposed by BMP-2 stimulation.

From a broader perspective, this coupling between integrins and BMPR signaling pathways is of great relevance in developmental processes and regenerative medicine, where cell recruitment is a prerequisite to cell differentiation to form a

Downloaded from jcb.rupress.org on March 7, 2016

Published March 7, 2016

specific organ or repair damaged tissue. Identification of signaling pathways such as the β3 integrin–GSK3 axis here and tools to control β3 integrin and GSK3 activities via engineered biomaterials and/or pharmacological agents would provide new therapeutic strategies for optimizing bone repair and regeneration.

## Materials and methods

### Buildup of PLL/HA films, cross-linking, and loading of rhBMP-2

Sodium hyaluronate (HA; $2 \times 10^5$ g/mol) was purchased from Lifecore Biomedical, and PLL ($2 \times 10^4$ g/mol) was purchased from Sigma-Aldrich. PLL (0.5 mg/ml) and HA (1 mg/ml) were dissolved in a Hepes-NaCl buffer (20 mM Hepes, pH 7.4, and 0.15 M NaCl). For all experiments, $(PLL/HA)_{12}$ films (i.e., made of 12-layer pairs of PLL and HA) were prepared as previously described (Crouzier et al., 2009) with a dipping machine (Dipping Robot DR3; Kierstein) on 14-mm- or 32-mm-diameter glass slides (VWR Scientific). For quantification of cell adhesion, the films were manually constructed in 96-well plates (Nunc) starting with a first layer of poly(ethyleneimine) ($7 \times 10^4$ g/mol; Sigma-Aldrich) at 3 mg/ml. In brief, polyelectrolyte solutions (50 µl) were deposited in each well and left to adsorb for 8 min before being washed twice with rinsing solution (100 µl 0.15 M NaCl, pH ∼6) for 1 min. The sequence was repeated until the buildup of a $(PLL/HA)_{12}$ film was achieved. The films were CL following the protocol previously described using 1-ethyl-3-(3-dimethylamino-propyl)carbodiimide at 30 mg/ml (soft films) or 70 mg/ml (stiff films) and *N*-hydrosulfosuccinimide at 11 mg/ml (both purchased from Sigma-Aldrich; Crouzier et al., 2009).

BMP-2 (clinical grade; Medtronic) was incorporated into films preequilibrated for 30 min in the medium in which BMP-2 was suspended (1 mM HCl). It was deposited onto the films and left to adsorb overnight at 4°C. The coated slides were thoroughly washed for 1 h in Hepes-NaCl to keep only matrix-bound BMP-2 (Crouzier et al., 2009) before being sterilized for 15 min under UV light. The experiments were performed at least three times, with at least three triplicate samples per condition in each experiment.

Mechanical properties of the films were characterized by nanoindentation with a colloidal probe using atomic force microscopy as described previously (Boudou et al., 2011). The force–indentation curves were fitted by a modified Hertz model to take into account the finite film thickness.

### Cells and reagents

C2C12 cells and mesenchymal stem cells (D1MSC, <20 passages; ATCC) were maintained in polystyrene flasks in a 37°C, 5% $CO_2$ incubator, and cultured in a 1:1 DMEM/F12 medium and α-MEM, respectively (Gibco and Invitrogen) supplemented with 10% FBS (PAA Laboratories) containing 10 U/ml penicillin G and 10 µg/ml streptomycin (Gibco and Invitrogen; growth medium [GM]). Cells were subcultured before reaching 60–70% confluence (approximately every 2 d). For all experiments, C2C12 cells seeded on films at $1.5 \times 10^4$ cells/cm$^2$ in growth medium were allowed to grow for 4 h. A full list of the inhibitors used as well as their working concentration can be found in Table S2. After dissolution in DMSO, they were added into the medium at the same time as cell plating on films.

Hamster anti-$\alpha_5$, rat anti-$\beta_1$, and hamster anti–β3 integrin blocking antibodies were purchased from BD. Hamster anti-$\alpha_V$ blocking antibody was purchased from Santa Cruz Biotechnology (Tebu-Bio). For immuno-fluorescence, anti-$\alpha_5$ and rat anti-$\beta_1$ were purchased from Chemicon (EMD Millipore). Hamster anti-$\alpha_V$ and hamster anti-β3 were purchased from Santa Cruz Biotechnology, Inc. Phalloidin-TRITC, mouse anti-vinculin, and rabbit anti-FN were purchased from Sigma-Aldrich. Rabbit anti-Smad1 and rabbit anti-pSmad1,5,8 were purchased from Cell Signaling Technology. Alexa Fluor–conjugated secondary antibodies and Hoechst 33342 were purchased from Invitrogen. 3,3′-dithiobis-sulfosuccinimidylpropionate (DTSSP) was from Pierce (Thermo Fischer Scientific). Antibodies used for Western blotting were rabbit anti-Smad1 (Cell Signaling Technology) rabbit anti-phosphoSmad1,5,8 (Cell Signaling Technology), rabbit anti-GAD PH (Cell Signaling Technology), rabbit anti–phospo-GSK3β (Cell Signaling Technology), homemade rabbit anti–β1 integrin (Albiges-Rizo laboratory), rat anti–β3 integrin (Emfret Analytics), and mouse anti-actin (Sigma-Aldrich). Cyclic RGD peptide and negative control cRAD were purchased from AnaSpec (Tebu-Bio).

### Quantification of cell adhesion and integrin binding assays

The cell-counting tests were performed in 96-well plates. The cell numbers were assessed after 4 h of adhesion using a cell-counting kit (CyQUANT, Molecular Probes, and Invitrogen). In brief, the cells were washed three times with PBS and frozen at −80°C overnight. After thawing the cells at RT, a mixture of the CyQUANT GR dye and cell-lysis buffer was introduced and the fluorescence of the plates was measured using the Tecan Infinite 1000 spectrofluorimeter (excitation 485/emission 535; Tecan). For inhibition of initial adhesion by anti-integrin antibodies, cells ($10^5$ cells/ml) were pretreated with either anti–β or anti–α integrin subunits at 10 µg/ml for 30 min at 37°C. The cells in the presence of antibodies were then seeded onto the surfaces at $10^4$ cells/cm$^2$. For integrin activation with $Mn^{2+}$, $MnCl_2$ at 0.5 mM was directly added to the cell suspension during the adhesion phase for 1 or 4 h (Cluzel et al., 2005).

### Immunofluorescence

For staining of F-actin, vinculin, FN, Smad1, and pSmad1,5,8, cells were fixed in 3.7% formaldehyde in PBS for 20 min and permeabilized for 4 min in TBS (0.15 M NaCl and 50 mM Tris-HCl, pH 7.4) containing 0.2% Triton X-100. After rinsing with PBS, samples were incubated for 1 h in 0.1% BSA in TRIS-buffered saline (50 mM TRIS, 150 mM NaCl, 0.1% $NaN_3$, pH 7.4). Actin was labeled with phalloidin-TRITC for 30 min. Cell nuclei were stained with 5 µg/ml Hoechst 33342 for 10 min. After the incubations with the primary antibodies (diluted in 0.2% TBS-gelatin) for 30 min at RT, cells were washed three times in TBS and incubated for 30 min with the secondary antibodies.

For $\alpha_5$ and $\alpha_V$, $\beta_1$, and $\beta_3$ integrin staining, a protocol adapted from that of Keselowsky et al. (2005) was used. In brief, cells were rinsed in PBS and incubated in ice-cold DTSSP (in 1 mM final concentration in PBS) for 30 min. Unreacted cross-linker was quenched with 50 mM Tris in PBS for 15 min and bulk cellular components were extracted in 0.1% SDS in PBS. The slides were then blocked in 0.1% BSA in TBS. After this, bound integrins were immunostained with antibodies against α or β chains and Alexa Fluor 488–conjugated secondary antibody. All the slides were mounted onto coverslips with antifade reagent (Prolong; Invitrogen) and viewed under fluorescence microscopy (LSM 710, Axiovert 200M; ZEISS) using a 10×/0.25 NA, 20×/0.8 NA, or 63×/1.4 NA objectives. Images were acquired with Metaview software using a CoolSNAP EZ CCD camera (Roper Technologies). To quantify cell spreading, fluorescence images were analyzed with the ImageJ software to determine mean cell area.

### siRNA interference

Cells were transfected with siRNA against $\beta_1$ or $\beta_3$ integrins, BMP receptor Ia or II, Src, FAK, ILK, Cdc42, ROCK1&2, or FN (ON-TARGET plus SMARTpool; respectively, mouse ITGB1, ITGB3, BMPR-Ia, and BMPR-II, Src, Ptk2, Cdc42, ILK, Rock1 and Rock2, and FN; Thermo

Downloaded from jcb.rupress.org on March 7, 2016

Published March 7, 2016

Fisher Scientific and GE Healthcare). The gene target SiRNA sequences used for transfection are listed in Table S3. A scrambled siRNA (all stars negative control siRNA; QIAGEN) was taken as control. Cells were seeded at 5,000 cells/cm$^2$ in six-well plates and cultured in 2 ml of GM for 15 h. The transfection mix was prepared as follows: For one well, 6 µl of Lipofectamine RNAiMAX Reagent (Invitrogen) was added to 305 µl of Opti-MEM medium (Gibco) and 0.72 µl of 1 mM siRNA was added to another 305 µl Opti-MEM medium. Lipofectamine-containing mix was added to siRNA-containing mix and incubated for 20 min at RT. Before transfection, the GM of the wells was replaced by the GM without antibiotics. Then, 610 µl of the final mix was added to each well. After 24 h of incubation at 37°C, the cells were transfected for the second time and incubated for another 24 h. The cells were then detached by trypsin-EDTA, seeded in GM at 15,000 cells/cm$^2$ on the films, and allowed to adhere for 4 h.

### Smad assay using Luciferase reporter gene

C2C12 stably transfected with an expression construct (BRE-Luc) containing a BMP-responsive element fused to the firefly luciferase reporter gene (Logeart-Avramoglou et al., 2006) were used (gift from D. Logeart-Avramoglou, Paris Diderot University, Paris, France). They were cultured under the same conditions as nontransfected C2C12 cells. After 15 h of culture on the films, cell lysis and luciferase measurements were performed according to the manufacturer's instructions (Bright-Glo luciferase assay system; Promega). As the luciferase signal is increasing as a function of time by displaying a sixfold higher signal at 24 h than at 4 h (250 versus 1,600 arbitrary units), the time point of 15 h was selected for luciferase treatment to be able to quantify the effect of drugs or SiRNA.

Measurements were normalized to the DNA content of each sample as measured by the CyQUANT assay. The effect on various drugs on BMP pathway was assessed in 96-well plates using 15,000 cells/cm$^2$ and drugs at various concentrations.

### Measurement of ALP activity in C2C12

After 3 d in culture on BMP-2 loaded films in 96-well plates, C2C12 cells were assayed for ALP activity, a marker for osteoblast differentiation. After removal of culture medium, cells were lysed by adding a 50 µl of 0.5% Triton-X100 in PBS supplemented with 0.15 µl benzonase (Novagen) and 1× antiprotease (antiprotease complete; Roche). The plate was put at 37°C for 20 min, and half of the volume was conserved for the protein assay. A buffer containing 0.1 M 2-amino-2-methyl-l-propanol (Sigma-Aldrich), 1 mM $MgCI_2$, and 9 mM *p*-nitrophenol phosphate (Euromedex), adjusted to pH 10.0 with HCl, was used to assay the cell lysate for ALP. Reaction was followed over 5 min in a 96-well plate by measuring the absorbance at 405 nm using a Tecan Infinite 1000 Microplate reader. The activity was expressed as µmoles of p-nitrophenol produced per minute per milligram of protein. Total protein contents of the samples were determined using a BCA protein assay kit (Interchim).

### Immunoblotting

Cells were lysed in Laemmli buffer. Detection of proteins by Western blotting was done according to standard protocols. After electrotransfer and blocking (10 mM Tris, pH 7.9, 150 mM NaCl, 0.5% Tween 20, and 3% dry milk at RT for 1 h), the PVDF membrane was incubated with antibodies overnight at 4°C. Immunological detection was achieved with HRP-conjugated secondary antibody. Peroxidase activity was visualized by ECL (West pico signal; Thermo Fisher Scientific) using a ChemiDoc MP imaging system (Bio-Rad Laboratories). Densitometric quantification of the bands was performed using the Image Lab program (Bio-Rad Laboratories). As control, detection of actin was also performed.

### Quantitative PCR

For RNA reverse-transcription and real-time quantitative PCR, total RNA was prepared from C2C12 myoblasts after cell lysis using a kit (Zymo Research). After reverse transcription of 1 µg total RNA, PCR was performed using a set of gene specific primers for FN and collagen. The sequences of primers used for real time PCR are listed in Table S4. cDNA (equivalent to 10 ng) was used for real-time quantitative PCR, performed with a thermocycler (MX4800P; Agilent Technologies). The 12-µl reaction mix contained 1-µl Master SYBR Green I mix, including Taq DNA polymerase, buffer, deoxynucleoside trisphosphate mix, SYBR Green I dye, 3 mM $MgCl_2$, and 0.5 µM of each primer. 2 µl of 30-fold-diluted cDNA was added to the mixture. Primer efficiency was established by a standard curve using sequential dilutions of gene-specific PCR fragments. Data were normalized from the quantitative RT-PCR housekeeping gene ATP50 as an index of cDNA content after reverse transcription.

### Time-lapse image acquisition

Cells were plated on either low- or high-CL films without BMP-2 or with sBMP-2 or bBMP-2 in standard GM at 37°C in 5% $CO_2$. Time-lapse images were acquired every 15 min over a 16-h period (after the initial 4-h adhesion period) using a 10×/0.3 NA objective in phase-contrast microscopy (Axiovert 200M; ZEISS). Images were acquired with Metaview software using a CoolSNAP HQ2 CCD camera (Roper Scientific). Migration velocities were measured using "Manual Tracking" and "Chemotaxis and Migration Tool" plugins from ImageJ. For both analyses, at least 60 cells were analyzed for each time point.

### FRAP experiment

C2C12 cells transfected with EGFP-paxillin were cultured on stiff film with sBMP-2 or bBMP-2 12 h before the experiment. FRAP experiments were performed in standard GM at 37°C in 5% $CO_2$. with a confocal microscope (LSM710; ZEISS) using a 63× objective (Plan-Apochromat 63×/1.4 oil DICIII, WD 190) equipped with on-stage incubator. One 0.03-µm$^2$ area located in the center of one focal adhesion was processed by FRAP. EGFP fluorescence in this adhesion area was eliminated by 10 bleach cycles at 100% intensity of the 488-nm argon laser. The fluorescence recovery was then sampled with low laser power (3%) each 5 s for 3 min. The recovery curves were obtained using Zen software. The corrected curve was adjusted with origin software using monoexponential fit. The characteristic recovery time ($\tau$) of EGFP-paxillin deduced from the fit of the experimental data was the mean of at least 20 individual focal adhesions.

### Scanning electron microscopy imaging

Cells grown on low-CL films for 4 h were fixed in 2.5% glutaraldehyde, 0.1 M sodium cacodylate, and 0.1 M sucrose, pH 7.2. Samples were then gradually dehydrated using increasing concentrations of ethanol mixtures up to 100%. Before imaging, the samples were air-dried and then carbon-coated. The samples were observed using a Quanta 250 Field emission gun SEM (FEI Company) at 5 kV equipped with a high-contrast backscatter detector.

### Lifetime of Smad1 and phospho-Smad1,5,8 measurement

C2C12 cells depleted or not with β3 integrin were seeded at 30,000 cells/cm$^2$ in six-well plates. After 4 h ($t = 0$), cells were incubated with 100 µg/ml cycloheximide and 600 ng/ml BMP-2. After the indicated time, cells were lysed and the phospho-Smad1,5,8 and Smad1 protein contents in the total lysates were visualized by Western blotting.

Downloaded from jcb.rupress.org on March 7, 2016

Published March 7, 2016

### Statistical analysis

Error bars represent standard errors, and statistical analysis was performed using Sigma-Plot v12.5 software. Student's *t* test was used to evaluate the statistical differences between two samples. For cell spreading and FRAP experiments, the Mann-Whitney rank sum test was used. Statistical significance was determined at $\alpha = 0.05$ (NS, not significant; *, $P \leq 0.05$; **, $P \leq 0.005$).

### Online supplemental material

Fig. S1 shows the increase of BMP-2 potency when bound to matrix. Fig. S2 shows how Low CL film without BMP-2 provides inadequate adhesion for C2C12 cells and identification of αv integrins as important receptors to mediate BMP-2–induced cell spreading. Fig. S3 shows that bBMP-2 does not induce the expression of FN and collagen but cell spreading depends on bBMP2 and FN. Fig. S4 shows the control of nuclear localization of Smad by Src, FAK, and LIMK. Fig. S5 shows the involvement of β3 integrin and BMPR in Smad and GSK3 phosphorylations in both C2C12 and D1 MSC cells. Table S1 shows the physicochemical properties of (PLL/HA) films loaded or not with bBMP-2. Table S2 gives the list of inhibitors used to interfere with BMPR receptor and β3 integrin signaling, their working concentration and provider. Table S3 gives the list of the gene target siRNA sequences used for transfection. Table S4 gives the primer sequences used for quantitative PCR experiments. Online supplemental material is available at http://www.jcb.org/cgi/content/full/jcb.201508018/DC1.

## Acknowledgments

We thank D. Logeart-Avramoglou for providing the C2C12-A5–transfected cells; P. Knaus, S. Bailly, and F. Bruckert for fruitful discussions; and M. Billaud, J. Almodovar, T. Boudou, and E. Van Obberghen-Schilling for comments on the manuscript. We thank C. Oddou, A.-S. Riba, M. Regent, M. Mignot, F. Gilde, and C. Fournier for their technical help.

This work was supported by the European Commission, FP7, via a European Research Council starting grant to C. Picart (BIOMIM, GA 239370), by the Institut Universitaire de France (C. Picart), by the Fondation pour la Recherche Médical (C. Albiges-Rizo), and by the Ligue Contre le Cancer for Equipe labelisée Ligue 2014 (C. Albiges-Rizo). The groups of C. Picart and C. Albiges-Rizo belong to the Centre National de la Recherche Scientifique consortium CellTiss.

The authors declare no competing financial interests.

Submitted: 6 August 2015
Accepted: 9 February 2016

## References

Albiges-Rizo, C., O. Destaing, B. Fourcade, E. Planus, and M.R. Block. 2009. Actin machinery and mechanosensitivity in invadopodia, podosomes and focal adhesions. *J. Cell Sci.* 122:3037–3049. http://dx.doi.org/10.1242/jcs.052704

Aragón, E., N. Goerner, A.-I. Zaromytidou, Q. Xi, A. Escobedo, J. Massagué, and M.J. Macias. 2011. A Smad action turnover switch operated by WW domain readers of a phosphoserine code. *Genes Dev.* 25:1275–1288. http://dx.doi.org/10.1101/gad.2060811

Biver, E., C. Thouverey, D. Magne, and J. Caverzasio. 2014. Crosstalk between tyrosine kinase receptors, GSK3 and BMP2 signaling during osteoblastic differentiation of human mesenchymal stem cells. *Mol. Cell. Endocrinol.* 382:120–130. http://dx.doi.org/10.1016/j.mce.2013.09.018

Boudou, T., T. Crouzier, C. Nicolas, K. Ren, and C. Picart. 2011. Polyelectrolyte multilayer nanofilms used as thin materials for cell mechano-sensitivity studies. *Macromol. Biosci.* 11:77–89. http://dx.doi.org/10.1002/mabi.201000301

Brakebusch, C., and R. Fässler. 2003. The integrin-actin connection, an eternal love affair. *EMBO J.* 22:2324–2333. http://dx.doi.org/10.1093/emboj/cdg245

Capdevila, J., and J.C. Izpisúa Belmonte. 2001. Patterning mechanisms controlling vertebrate limb development. *Annu. Rev. Cell Dev. Biol.* 17:87–132. http://dx.doi.org/10.1146/annurev.cellbio.17.1.87

Chen, T.T., A. Luque, S. Lee, S.M. Anderson, T. Segura, and M.L. Iruela-Arispe. 2010. Anchorage of VEGF to the extracellular matrix conveys differential signaling responses to endothelial cells. *J. Cell Biol.* 188:595–609. http://dx.doi.org/10.1083/jcb.200906044

Cheng, S.L., F. Lecanda, M.K. Davidson, P.M. Warlow, S.F. Zhang, L. Zhang, S. Suzuki, T. St John, and R. Civitelli. 1998. Human osteoblasts express a repertoire of cadherins, which are critical for BMP-2-induced osteogenic differentiation. *J. Bone Miner. Res.* 13:633–644. http://dx.doi.org/10.1359/jbmr.1998.13.4.633

Cluzel, C., F. Saltel, J. Lussi, F. Paulhe, B.A. Imhof, and B. Wehrle-Haller. 2005. The mechanisms and dynamics of (alpha)v(beta)3 integrin clustering in living cells. *J. Cell Biol.* 171:383–392. http://dx.doi.org/10.1083/jcb.200503017

Comoglio, P.M., C. Boccaccio, and L. Trusolino. 2003. Interactions between growth factor receptors and adhesion molecules: breaking the rules. *Curr. Opin. Cell Biol.* 15:565–571. http://dx.doi.org/10.1016/S0955-0674(03)00096-6

Crouzier, T., K. Ren, C. Nicolas, C. Roy, and C. Picart. 2009. Layer-by-layer films as a biomimetic reservoir for rhBMP-2 delivery: controlled differentiation of myoblasts to osteoblasts. *Small.* 5:598–608. http://dx.doi.org/10.1002/smll.200800804

Crouzier, T., L. Fourel, T. Boudou, C. Albigès-Rizo, and C. Picart. 2011a. Presentation of BMP-2 from a soft biopolymeric film unveils its activity on cell adhesion and migration. *Adv. Mater.* 23:H111–H118. http://dx.doi.org/10.1002/adma.201004637

Crouzier, T., F. Sailhan, P. Becquart, R. Guillot, D. Logeart-Avramoglou, and C. Picart. 2011b. The performance of BMP-2 loaded TCP/HAP porous ceramics with a polyelectrolyte multilayer film coating. *Biomaterials.* 32:7543–7554. http://dx.doi.org/10.1016/j.biomaterials.2011.06.062

Dechantsreiter, M.A., E. Planker, B. Mathä, E. Lohof, G. Hölzemann, A. Jonczyk, S.L. Goodman, and H. Kessler. 1999. N-Methylated cyclic RGD peptides as highly active and selective α(V)β(3) integrin antagonists. *J. Med. Chem.* 42:3033–3040. http://dx.doi.org/10.1021/jm970832g

Delcommenne, M., C. Tan, V. Gray, L. Rue, J. Woodgett, and S. Dedhar. 1998. Phosphoinositide-3-OH kinase-dependent regulation of glycogen synthase kinase 3 and protein kinase B/AKT by the integrin-linked kinase. *Proc. Natl. Acad. Sci. USA.* 95:11211–11216. http://dx.doi.org/10.1073/pnas.95.19.11211

Dingal, P.C.D.P., A.M. Bradshaw, S. Cho, M. Raab, A. Buxboim, J. Swift, and D.E. Discher. 2015. Fractal heterogeneity in minimal matrix models of scars modulates stiff-niche stem-cell responses via nuclear exit of a mechanorepressor. *Nat. Mater.* 14:951–960. http://dx.doi.org/10.1038/nmat4350

Discher, D.E., P. Janmey, and Y.L. Wang. 2005. Tissue cells feel and respond to the stiffness of their substrate. *Science.* 310:1139–1143. http://dx.doi.org/10.1126/science.1116995

Discher, D.E., D.J. Mooney, and P.W. Zandstra. 2009. Growth factors, matrices, and forces combine and control stem cells. *Science.* 324:1673–1677. http://dx.doi.org/10.1126/science.1171643

Dopie, J., K.-P. Skarp, E.K. Rajakylä, K. Tanhuanpää, and M.K. Vartiainen. 2012. Active maintenance of nuclear actin by importin 9 supports transcription. *Proc. Natl. Acad. Sci. USA.* 109:E544–E552. http://dx.doi.org/10.1073/pnas.1118880109

Dudas, M., S. Sridurongrit, A. Nagy, K. Okazaki, and V. Kaartinen. 2004. Craniofacial defects in mice lacking BMP type I receptor Alk2 in neural crest cells. *Mech. Dev.* 121:173–182. http://dx.doi.org/10.1016/j.mod.2003.12.003

Engler, A.J., S. Sen, H.L. Sweeney, and D.E. Discher. 2006. Matrix elasticity directs stem cell lineage specification. *Cell.* 126:677–689. http://dx.doi.org/10.1016/j.cell.2006.06.044

Fan, V.H., K. Tamama, A. Au, R. Littrell, L.B. Richardson, J.W. Wright, A. Wells, and L.G. Griffith. 2007. Tethered epidermal growth factor provides a survival advantage to mesenchymal stem cells. *Stem Cells.* 25:1241–1251. http://dx.doi.org/10.1634/stemcells.2006-0320

Foletta, V.C., M.A. Lim, J. Soosairajah, A.P. Kelly, E.G. Stanley, M. Shannon, W. He, S. Das, J. Massague, O. Bernard, and J. Soosairaiah. 2003. Direct signaling by the BMP type II receptor via the cytoskeletal regulator LIMK1. *J. Cell Biol.* 162:1089–1098. http://dx.doi.org/10.1083/jcb.200212060

Fuentealba, L.C., E. Eivers, A. Ikeda, C. Hurtado, H. Kuroda, E.M. Pera, and E.M. De Robertis. 2007. Integrating patterning signals: Wnt/GSK3 regulates the duration of the BMP/Smad1 signal. *Cell.* 131:980–993. http://dx.doi.org/10.1016/j.cell.2007.09.027

Downloaded from jcb.rupress.org on March 7, 2016

Published March 7, 2016

Gamell, C., N. Osses, R. Bartrons, T. Rückle, M. Camps, J.L. Rosa, and F. Ventura. 2008. BMP2 induction of actin cytoskeleton reorganization and cell migration requires PI3-kinase and Cdc42 activity. *J. Cell Sci.* 121:3960–3970. http://dx.doi.org/10.1242/jcs.031286

Gilbert, P.M., J.K. Mouw, M.A. Unger, J.N. Lakins, M.K. Gbegnon, V.B. Clemmer, M. Benezra, J.D. Licht, N.J. Boudreau, K.K.C. Tsai, et al. 2010. HOXA9 regulates BRCA1 expression to modulate human breast tumor phenotype. *J. Clin. Invest.* 120:1535–1550. http://dx.doi.org/10.1172/JCI39534

Goldstein, A.M., K.C. Brewer, A.M. Doyle, N. Nagy, and D.J. Roberts. 2005. BMP signaling is necessary for neural crest cell migration and ganglion formation in the enteric nervous system. *Mech. Dev.* 122:821–833. http://dx.doi.org/10.1016/j.mod.2005.03.003

Hanna, S., and M. El-Sibai. 2013. Signaling networks of Rho GTPases in cell motility. *Cell. Signal.* 25:1955–1961. http://dx.doi.org/10.1016/j.cellsig.2013.04.009

Huttenlocher, A., and A.R. Horwitz. 2011. Integrins in cell migration. *Cold Spring Harb. Perspect. Biol.* 3:a005074. http://dx.doi.org/10.1101/cshperspect.a005074

Hynes, R.O. 2009. The extracellular matrix: not just pretty fibrils. *Science.* 326:1216–1219. http://dx.doi.org/10.1126/science.1176009

Ivaska, J., and J. Heino. 2011. Cooperation between integrins and growth factor receptors in signaling and endocytosis. *Annu. Rev. Cell Dev. Biol.* 27:291–320. http://dx.doi.org/10.1146/annurev-cellbio-092910-154017

Katagiri, T., A. Yamaguchi, M. Komaki, E. Abe, N. Takahashi, T. Ikeda, V. Rosen, J.M. Wozney, A. Fujisawa-Sehara, and T. Suda. 1994. Bone morphogenetic protein-2 converts the differentiation pathway of C2C12 myoblasts into the osteoblast lineage. *J. Cell Biol.* 127:1755–1766. http://dx.doi.org/10.1083/jcb.127.6.1755

Katagiri, T., S. Akiyama, M. Namiki, M. Komaki, A. Yamaguchi, V. Rosen, J.M. Wozney, A. Fujisawa-Sehara, and T. Suda. 1997. Bone morphogenetic protein-2 inhibits terminal differentiation of myogenic cells by suppressing the transcriptional activity of MyoD and myogenin. *Exp. Cell Res.* 230:342–351. http://dx.doi.org/10.1006/excr.1996.3432

Keselowsky, B.G., D.M. Collard, and A.J. García. 2005. Integrin binding specificity regulates biomaterial surface chemistry effects on cell differentiation. *Proc. Natl. Acad. Sci. USA.* 102:5953–5957. http://dx.doi.org/10.1073/pnas.0407356102

King, W.J., and P.H. Krebsbach. 2012. Growth factor delivery: how surface interactions modulate release in vitro and in vivo. *Adv. Drug Deliv. Rev.* 64:1239–1256. http://dx.doi.org/10.1016/j.addr.2012.03.004

Kopf, J., P. Paarmann, C. Hiepen, D. Horbelt, and P. Knaus. 2014. BMP growth factor signaling in a biomechanical context. *Biofactors.* 40:171–187. http://dx.doi.org/10.1002/biof.1137

Krause, U., S. Harris, A. Green, J. Ylostalo, S. Zeitouni, N. Lee, and C.A. Gregory. 2010. Pharmaceutical modulation of canonical Wnt signaling in multipotent stromal cells for improved osteoinductive therapy. *Proc. Natl. Acad. Sci. USA.* 107:4147–4152. http://dx.doi.org/10.1073/pnas.0914360107

Logeart-Avramoglou, D., M. Bourguignon, K. Oudina, P. Ten Dijke, and H. Petite. 2006. An assay for the determination of biologically active bone morphogenetic proteins using cells transfected with an inhibitor of differentiation promoter-luciferase construct. *Anal. Biochem.* 349:78–86. http://dx.doi.org/10.1016/j.ab.2005.10.030

Lu, P., V.M. Weaver, and Z. Werb. 2012. The extracellular matrix: a dynamic niche in cancer progression. *J. Cell Biol.* 196:395–406. http://dx.doi.org/10.1083/jcb.201102147

Mammoto, T., and D.E. Ingber. 2010. Mechanical control of tissue and organ development. *Development.* 137:1407–1420. http://dx.doi.org/10.1242/dev.024166

Margadant, C., and A. Sonnenberg. 2010. Integrin-TGF-beta crosstalk in fibrosis, cancer and wound healing. *EMBO Rep.* 11:97–105. http://dx.doi.org/10.1038/embor.2009.276

Martino, M.M., F. Tortelli, M. Mochizuki, S. Traub, D. Ben-David, G.A. Kuhn, R. Müller, E. Livne, S.A. Eming, and J.A. Hubbell. 2011. Engineering the growth factor microenvironment with fibronectin domains to promote wound and bone tissue healing. *Sci. Transl. Med.* 3:100ra89. http://dx.doi.org/10.1126/scitranslmed.3002614

Martino, M.M., P.S. Briquez, E. Güç, F. Tortelli, W.W. Kilarski, S. Metzger, J.J. Rice, G.A. Kuhn, R. Müller, M.A. Swartz, and J.A. Hubbell. 2014. Growth factors engineered for super-affinity to the extracellular matrix enhance tissue healing. *Science.* 343:885–888. http://dx.doi.org/10.1126/science.1247663

Massagué, J. 2000. How cells read TGF-beta signals. *Nat. Rev. Mol. Cell Biol.* 1:169–178. http://dx.doi.org/10.1038/35043051

Massagué, J., and D. Wotton. 2000. Transcriptional control by the TGF-beta/Smad signaling system. *EMBO J.* 19:1745–1754. http://dx.doi.org/10.1093/emboj/19.8.1745

Mayer, U. 2003. Integrins: redundant or important players in skeletal muscle? *J. Biol. Chem.* 278:14587–14590. http://dx.doi.org/10.1074/jbc.R200022200

McBeath, R., D.M. Pirone, C.M. Nelson, K. Bhadriraju, and C.S. Chen. 2004. Cell shape, cytoskeletal tension, and RhoA regulate stem cell lineage commitment. *Dev. Cell.* 6:483–495. http://dx.doi.org/10.1016/S1534-5807(04)00075-9

Munsie, L.N., C.R. Desmond, and R. Truant. 2012. Cofilin nuclear-cytoplasmic shuttling affects cofilin-actin rod formation during stress. *J. Cell Sci.* 125:3977–3988. http://dx.doi.org/10.1242/jcs.097667

Nohe, A., S. Hassel, M. Ehrlich, F. Neubauer, W. Sebald, Y.I. Henis, and P. Knaus. 2002. The mode of bone morphogenetic protein (BMP) receptor oligomerization determines different BMP-2 signaling pathways. *J. Biol. Chem.* 277:5330–5338. http://dx.doi.org/10.1074/jbc.M102750200

Ozeki, N., P. Jethanandani, H. Nakamura, B.L. Ziober, and R.H. Kramer. 2007. Modulation of satellite cell adhesion and motility following BMP2-induced differentiation to osteoblast lineage. *Biochem. Biophys. Res. Commun.* 353:54–59. http://dx.doi.org/10.1016/j.bbrc.2006.11.110

Pelish, H.E., J.R. Peterson, S.B. Salvarezza, E. Rodriguez-Boulan, J.-L. Chen, M. Stamnes, E. Macia, Y. Feng, M.D. Shair, and T. Kirchhausen. 2006. Secramine inhibits Cdc42-dependent functions in cells and Cdc42 activation in vitro. *Nat. Chem. Biol.* 2:39–46. http://dx.doi.org/10.1038/nchembio751

Plotnikov, S.V., and C.M. Waterman. 2013. Guiding cell migration by tugging. *Curr. Opin. Cell Biol.* 25:619–626. http://dx.doi.org/10.1016/j.ceb.2013.06.003

Prudent, R., E. Vassal-Stermann, C.-H. Nguyen, C. Pillet, A. Martinez, C. Prunier, C. Barette, E. Soleilhac, O. Filhol, A. Beghin, et al. 2012. Pharmacological inhibition of LIM kinase stabilizes microtubules and inhibits neoplastic growth. *Cancer Res.* 72:4429–4439. http://dx.doi.org/10.1158/0008-5472.CAN-11-3342

Raftopoulou, M., and A. Hall. 2004. Cell migration: Rho GTPases lead the way. *Dev. Biol.* 265:23–32. http://dx.doi.org/10.1016/j.ydbio.2003.06.003

Ren, K., L. Fourel, C.G. Rouvière, C. Albiges-Rizo, and C. Picart. 2010. Manipulation of the adhesive behaviour of skeletal muscle cells on soft and stiff polyelectrolyte multilayers. *Acta Biomater.* 6:4238–4248. http://dx.doi.org/10.1016/j.actbio.2010.06.014

Sailer, M.H.M., T.G. Hazel, D.M. Panchision, D.J. Hoeppner, M.E. Schwab, and R.D.G. McKay. 2005. BMP2 and FGF2 cooperate to induce neural-crest-like fates from fetal and adult CNS stem cells. *J. Cell Sci.* 118:5849–5860. http://dx.doi.org/10.1242/jcs.02708

Sapkota, G., C. Alarcón, F.M. Spagnoli, A.H. Brivanlou, and J. Massagué. 2007. Balancing BMP signaling through integrated inputs into the Smad1 linker. *Mol. Cell.* 25:441–454. http://dx.doi.org/10.1016/j.molcel.2007.01.006

Schwartz, M.A. 2010. Integrins and extracellular matrix in mechanotransduction. *Cold Spring Harb. Perspect. Biol.* 2:a005066. http://dx.doi.org/10.1101/cshperspect.a005066

Sen, B., Z. Xie, G. Uzer, W.R. Thompson, M. Styner, X. Wu, and J. Rubin. 2015. Intranuclear Actin Regulates Osteogenesis. *Stem Cells.* 33:3065–3076. http://dx.doi.org/10.1002/stem.2090

Serrels, B., A. Serrels, V.G. Brunton, M. Holt, G.W. McLean, C.H. Gray, G.E. Jones, and M.C. Frame. 2007. Focal adhesion kinase controls actin assembly via a FERM-mediated interaction with the Arp2/3 complex. *Nat. Cell Biol.* 9:1046–1056. http://dx.doi.org/10.1038/ncb1626

Sieber, C., J. Kopf, C. Hiepen, and P. Knaus. 2009. Recent advances in BMP receptor signaling. *Cytokine Growth Factor Rev.* 20:343–355. http://dx.doi.org/10.1016/j.cytogfr.2009.10.007

Song, J., J. McColl, E. Camp, N. Kennerley, G.F. Mok, D. McCormick, T. Grocott, G.N. Wheeler, and A.E. Münsterberg. 2014. Smad1 transcription factor integrates BMP2 and Wnt3a signals in migrating cardiac progenitor cells. *Proc. Natl. Acad. Sci. USA.* 111:7337–7342. http://dx.doi.org/10.1073/pnas.1321764111

Swift, J., I.L. Ivanovska, A. Buxboim, T. Harada, P.C.D.P. Dingal, J. Pinter, J.D. Pajerowski, K.R. Spinler, J.-W. Shin, M. Tewari, et al. 2013. Nuclear lamin-A scales with tissue stiffness and enhances matrix-directed differentiation. *Science.* 341:1240104. http://dx.doi.org/10.1126/science.1240104

Tenney, R.M., and D.E. Discher. 2009. Stem cells, microenvironment mechanics, and growth factor activation. *Curr. Opin. Cell Biol.* 21:630–635. http://dx.doi.org/10.1016/j.ceb.2009.06.003

Tomar, A., and D.D. Schlaepfer. 2009. Focal adhesion kinase: switching between GAPs and GEFs in the regulation of cell motility. *Curr. Opin. Cell Biol.* 21:676–683. http://dx.doi.org/10.1016/j.ceb.2009.05.006

Downloaded from jcb.rupress.org on March 7, 2016

Published March 7, 2016

Tomar, A., and D.D. Schlaepfer. 2010. A PAK-activated linker for EGFR and FAK. *Dev. Cell.* 18:170–172. http://dx.doi.org/10.1016/j.devcel.2010.01.013

Vogel, V., and M. Sheetz. 2006. Local force and geometry sensing regulate cell functions. *Nat. Rev. Mol. Cell Biol.* 7:265–275. http://dx.doi.org/10.1038/nrm1890

Wang, Y.-K., X. Yu, D.M. Cohen, M.A. Wozniak, M.T. Yang, L. Gao, J. Eyckmans, and C.S. Chen. 2012. Bone morphogenetic protein-2-induced signaling and osteogenesis is regulated by cell shape, RhoA/ROCK, and cytoskeletal tension. *Stem Cells Dev.* 21:1176–1186. http://dx.doi.org/10.1089/scd.2011.0293

Yamamoto, N., S. Akiyama, T. Katagiri, M. Namiki, T. Kurokawa, and T. Suda. 1997. Smad1 and smad5 act downstream of intracellular signalings of BMP-2 that inhibits myogenic differentiation and induces osteoblast differentiation in C2C12 myoblasts. *Biochem. Biophys. Res. Commun.* 238:574–580. http://dx.doi.org/10.1006/bbrc.1997.7325

Yu, P.B., C.C. Hong, C. Sachidanandan, J.L. Babitt, D.Y. Deng, S.A. Hoyng, H.Y. Lin, K.D. Bloch, and R.T. Peterson. 2008. Dorsomorphin inhibits BMP signals required for embryogenesis and iron metabolism. *Nat. Chem. Biol.* 4:33–41. http://dx.doi.org/10.1038/nchembio.2007.54

Downloaded from jcb.rupress.org on March 7, 2016

Fourel et al., http://www.jcb.org/cgi/content/full/jcb.201508018/DC1

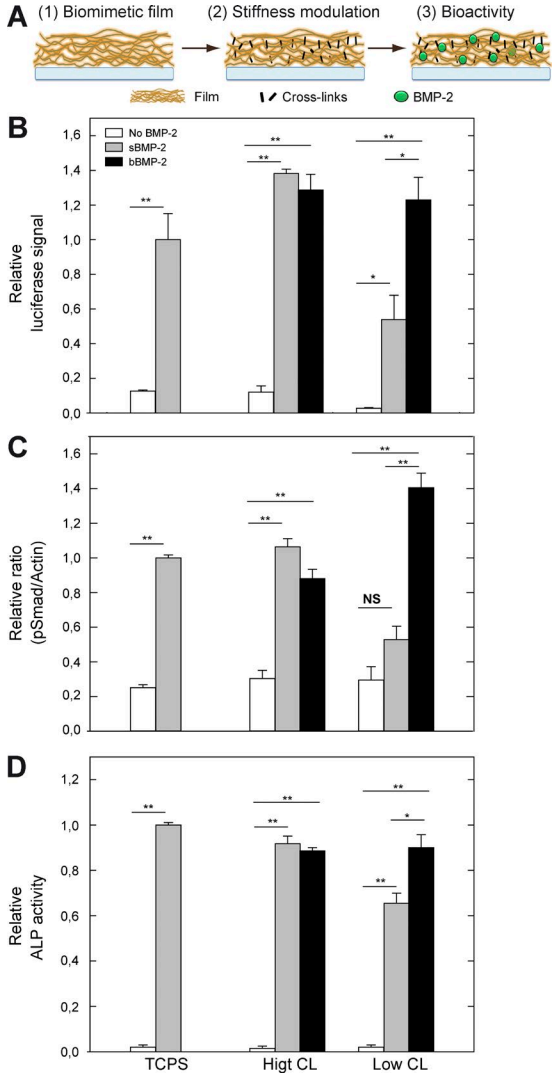



Figure S1. **BMP-2 potency is increased when bound to matrix.** (A) The biomaterial for the study of BMP-2 effects on cell behavior combines two functional properties of the tunable multilayer film system. (1) A polyelectrolyte multilayer film is built onto a substrate by alternating deposits of two polyelectrolytes: poly(L-lysine) and hyaluronan (PLL/HA). (2) The film can be covalently CL to different levels using a water-soluble carbodiimide, thus allowing film stiffness to be modulated. (3) BMP-2 is loaded into the film. BMP-2 is trapped in the film and delivered to the cells in a "matrix-bound" manner. (B) Luciferase activity of p(BRE) luciferase-transfected C2C12 cells was measured after 15 h of plating on tissue culture TCPS, soft PLL/HA film (Low CL), or PLL/HA stiff film (High CL) in the presence of soluble (sBMP-2) or matrix-bound BMP-2 (bBMP-2). (C) Western blot analysis of Smad activation using an anti–phospho-Smad1,5,8 antibody. The analysis of the intensity (ratio of phospho-Smad1,5,8/Actin) shows that phosphorylation of Smad occurs only when BMP-2 is present. (D) ALP expression after 4 d on soft and stiff films without or with BMP-2 shows that the signal is similar to that of soluble BMP-2 or higher in the case of the soft film. Experiments in B–D were performed three times. NS, not significant; *, $P \leq 0.05$; **, $P \leq 0.005$.



THE JOURNAL OF CELL BIOLOGY

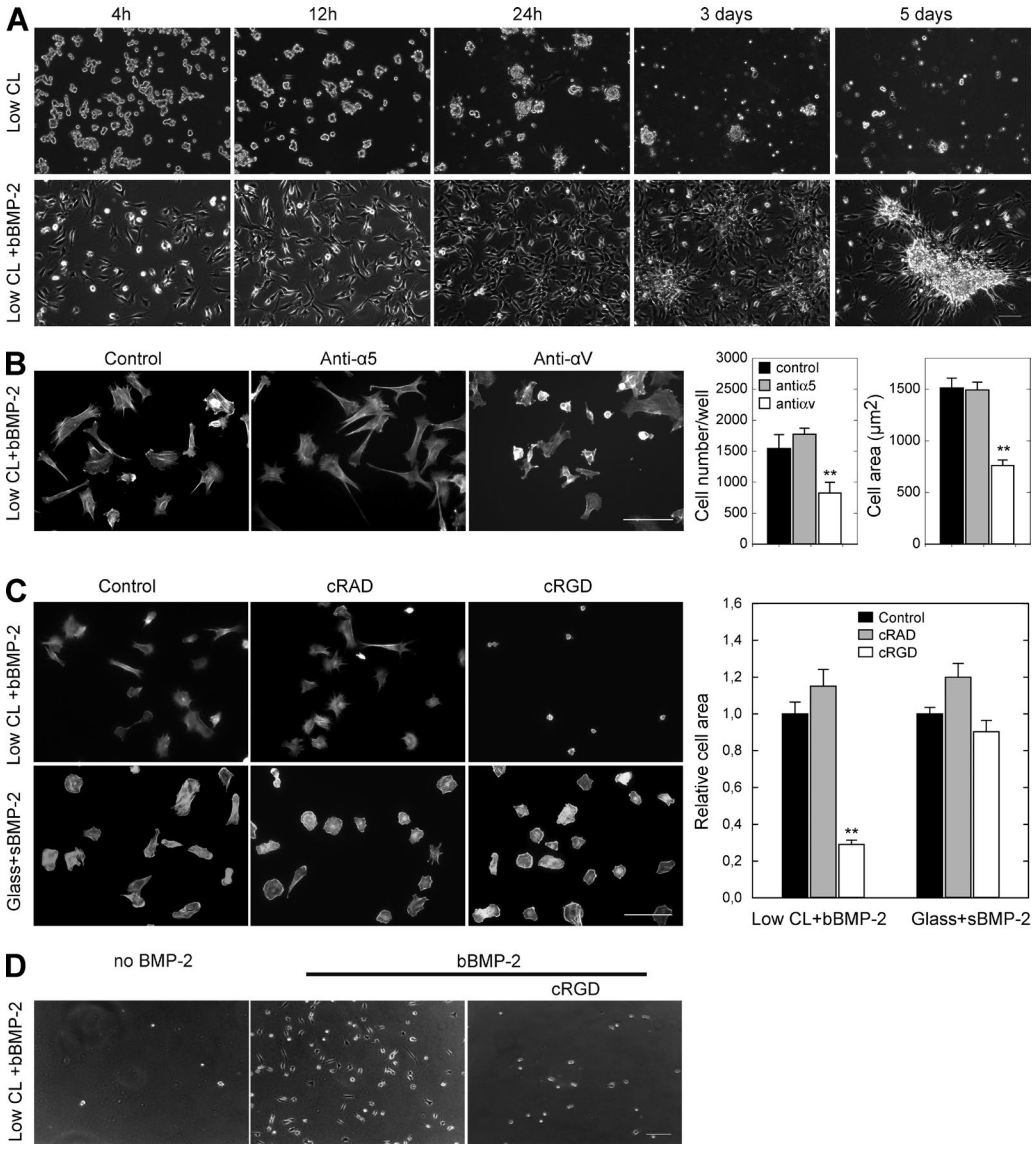



Figure S2. **αv integrins are required to mediate BMP-2-induced spreading.** (A) Low-CL film without BMP-2 provides inadequate adhesion for C2C12 cells. C2C12 cell spreading on low-CL films with bBMP-2 can be maintained for at least 24 h. At longer times, these cells tend to form cellular clusters and cohesive aggregates, which may be related to their osteogenic differentiation. (B) C2C12 cells were treated with blocking antibodies against α5 and αv chain integrins and plated for 4 h on low-CL film with bBMP-2. After 4 h, the number of adherent cells and cell spreading were quantified after labeling the actin cytoskeleton. The number of adherent cells and cell spreading area significantly decreased after treatment with antibodies against αv integrin on soft matrix–bound BMP-2. (C) C2C12 cell adhesion on low-CL film with bBMP-2 and on glass in the presence of cRAD and cRGD peptides in comparison to the control condition. Note the loss of C2C12 spreading upon treatment with cRGD. (D) D1 MSC adhesion onto low-CL film in the absence or presence of bBMP-2. D1 MSC cell spreading is blocked in the presence of cRGD. Data are means ± SEM from at least 60 cells per condition. Experiments were performed three times. **, $P \leq 0.005$ compared with control conditions. Bars, 100 μm.

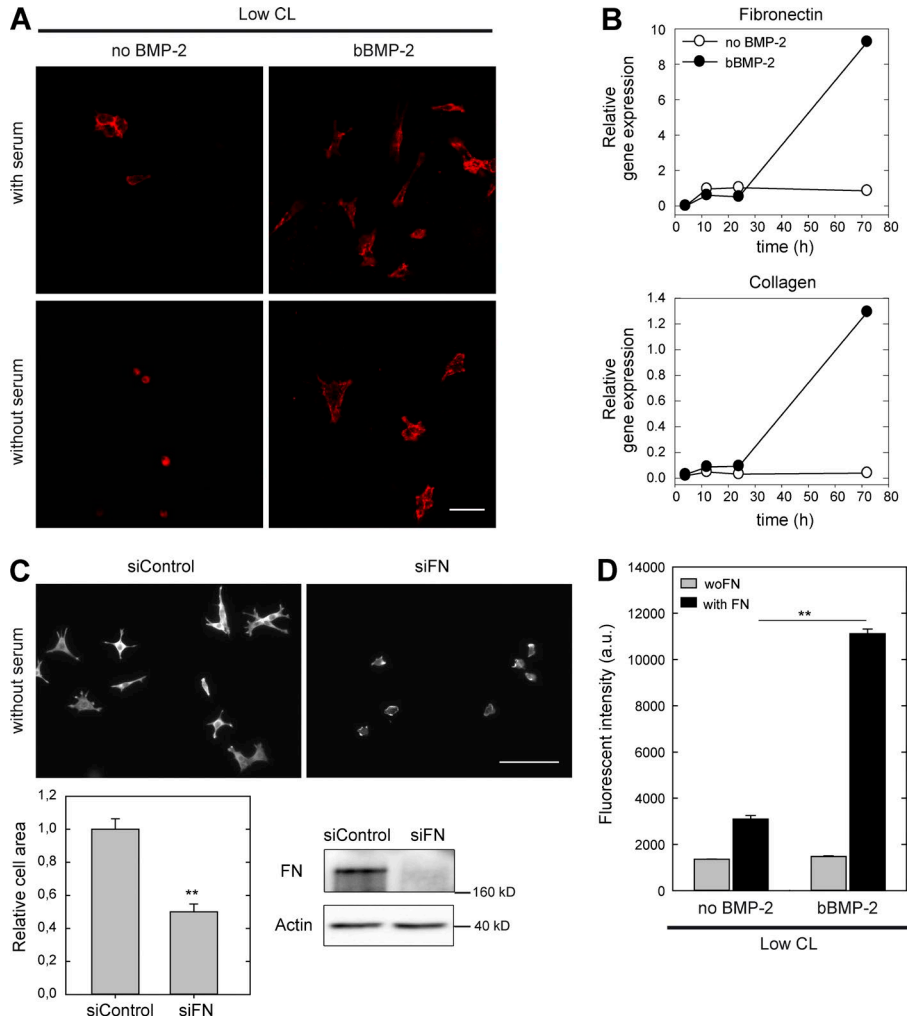



Figure S3. **BMP-2-bound matrix does not induce the expression of FN and collagen but cell spreading depends on bBMP2 and FN.** (A) Immunostaining of FN in cells grown on low-CL film without or with bBMP-2 for 4 h, in presence or absence of serum. (B) Quantitative PCR of FN and collagen mRNA expression shown over 72 h. (C) C2C12 cells were treated with SiRNA against FN and plated onto low-CL film with bBMP-2 before quantifying the relative cell area. The deletion of FN is controlled by Western blot. Data are means ± SEM from at least 60 cells per condition. (D) FN is preadsorbed or not on the low CL films without (wo) or with bBMP-2 and quantified by fluorescence spectroscopy after immunolabeling of the adsorbed FN. Data are means ± SEM ($n$ = 4); **, $P \leq 0.005$. Bars, 100 µm.

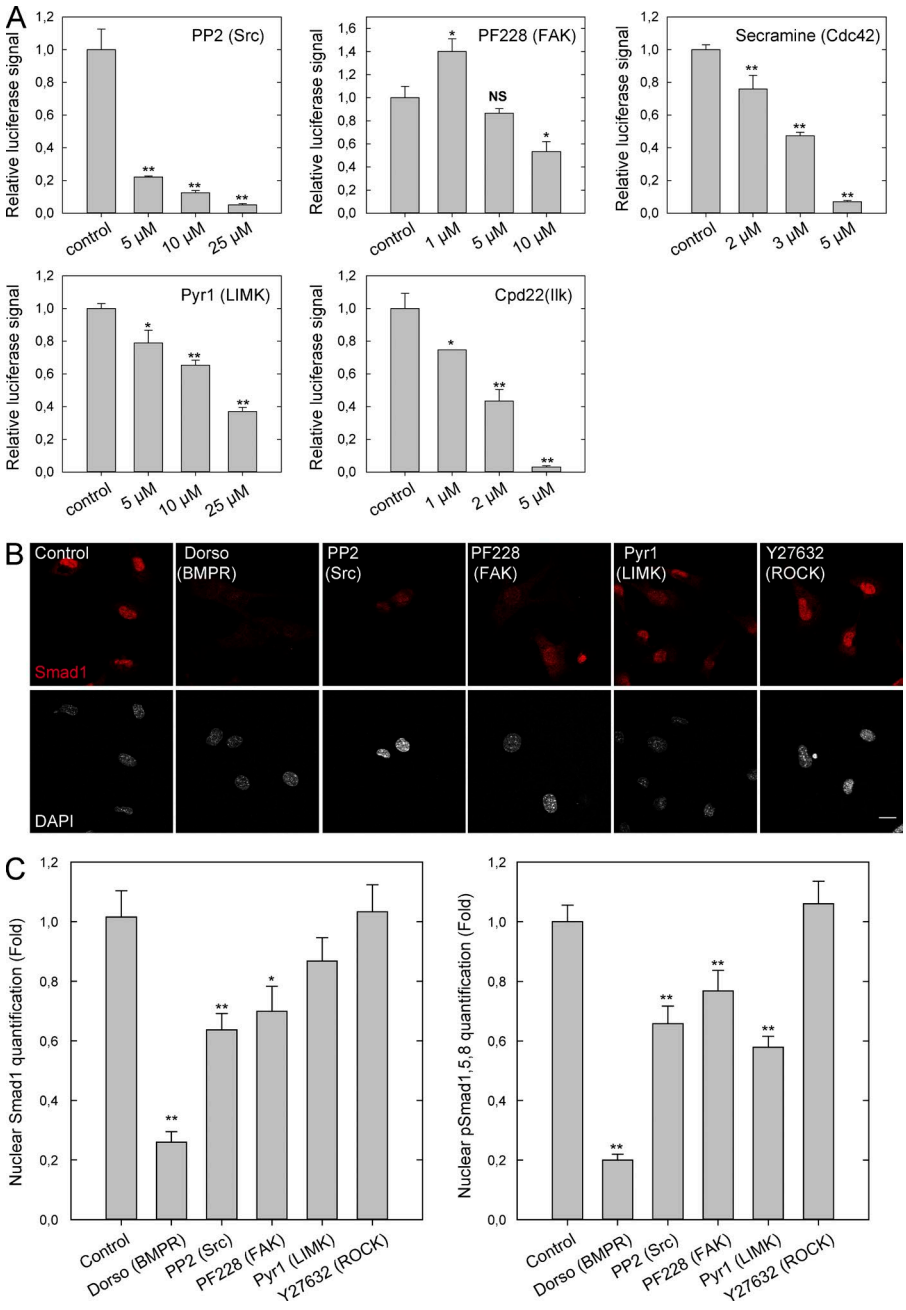



Figure S4. **Nuclear localization of Smad is controlled by Src, FAK, and LIMK.** (A) Dose-dependent effect of the inhibitors against Src, FAK, Cdc42, LIMK, and ILK. Luciferase activity of p(BRE) luciferase-transfected C2C12 cells was measured after 15 h plating on soft film with bBMP-2 in the presence of inhibitors with different concentrations. Data are means ± SEM ($n$ = 4). (B) Nuclear localization of Smad1 after 4 h on matrix-bound BMP-2 was observed by immunostaining in the presence of a series of inhibitors (dorsomorphin, PP2 [Src], PF228 [FAK], Pyr1 [LIMK], and Y27632 [ROCK]) as compared with control condition (DMSO); top: anti-Smad1; bottom: DAPI. (C) Quantification of nuclear Smad1 and pSmad1,5,8 in the absence or presence of inhibitors. Data are means ± SEM from at least 60 cells per condition. NS, not significant; *, $P \leq 0.05$; **, $P \leq 0.005$ as compared with control. Bar, 20 μm.

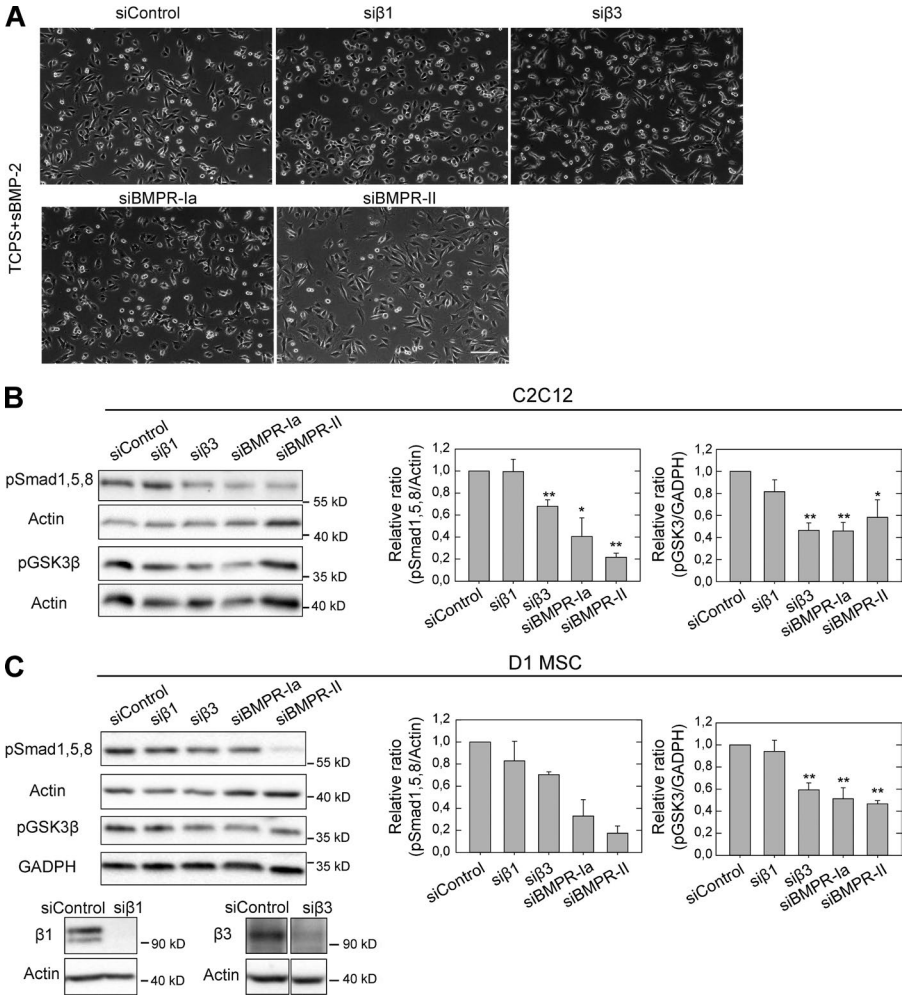



Figure S5. **Smad and GSK3 phosphorylations are dependent on β3 integrin and BMPR in both C2C12 and D1 MSC cells.** (A) Bright-field images of C2C12 cells after siRNA against β1integrin, β3 integrin, BMPR-Ia, and BMPR-II spread onto tissue culture polystyrene in presence of sBMP-2 for 4 h. C2C12 cells (B) or D1 MSC cells (C) are spread onto tissue culture polystyrene in presence of sBMP-2 for 4 h after depletion of β1 integrin, β3 integrin, BMPR-Ia, and BMPR-II to analyze by Western blot the level of Smad and GSK-3β activities using anti–phospho-Smad1,5,8 and phospho-GSK3β antibodies. Data are means ± SEM ($n$ = 3). The efficiency of β1 and β3 integrin deletion is validated by Western blot as shown in the bottom panel. *, $P \leq 0.05$; **, $P \leq 0.005$ as compared with control. Bar, 100 μm.

Table S1. **Physicochemical characteristics of soft and stiff films without or with bBMP-2**

| Characteristics | No BMP-2 | Matrix-bound BMP-2 |
|---|---|---|
| **Film stiffness $E_0$ (kPa)** | | |
| Low CL (soft films) | 182 ± 20 | 213 ± 34 |
| High CL (stiff films) | 358 ± 48 | 367 ± 58 |
| **Contact angle (°)** | | |
| Soft films | 43 ± 4 | 48 ± 4 |
| Stiff films | 48 ± 4 | 55 ± 7 |
| **Mean roughness (nm)** | | |
| Soft films | 4.2 ± 0.8 | 4.8 ± 0.2 |
| Stiff films | 6.8 ± 1.0 | 7.9 ± 0.4 |

Physical and chemical characteristics of soft or stiff $(PLL/HA)_{12}$ films without BMP-2 or in the presence of BMP-2 loaded in the films from a solution of 20 μg/ml. Film stiffness, contact angle, and film roughness were statistically similar without or with bBMP-2 ($P > 0.05$).

Table S2. **List of all pharmacological inhibitors and concentrations used**

| Target protein | Inhibitor | Manufacturer | Working concentration |
|---|---|---|---|
| | | | *μM* |
| LIMK | Pyr1 | Prudent et al., 2012 | 25 |
| ROCK | Y27632 | EMD Millipore | 10 |
| Rac | NSC 23766 | EMD Millipore | 100 |
| MLC | Blebbistatin | EMD Millipore | 5 |
| Rho A | C3 transferase | Cytoskeleton | 17 |
| BMPR/AMPK | Dorsomorphin | EMD Millipore | 10 |
| Src | PP2 | Sigma-Aldrich | 25 |
| Src | Number 5 | Biaffin | 10 |
| FAK | PF 228 | EMD Millipore | 10 |
| Cdc42 | Secramine | Pelish et al., 2006 | 5 |
| PI3K | LY294002 | Tocris Bioscience | 25 |
| ILK | Cpd22 | EMD Millipore | 2 |
| GSK3β | SB 216763 | Tocris Bioscience | 10 |
| F-actin | Cytochalasin D | EMD Millipore | 2 |
| F-actin | Latrunculin | EMD Millipore | 5 |

Table S3. **List of gene target siRNA sequences used for transfection**

| Gene target | Reference | siRNA target sequences (5′ to 3′) |
|---|---|---|
| BMPR-Ia | ON-TARGET plus SMARTpool, mouse BMPR-Ia (L-040598-00-0005; Thermo Scientific Dharmacon) | GAGGAAUCGUGGAGGAAUA GCUAGCUGGUUUAGAGAAA GAAAUGGCUCGUCGUUGUA GGCCAUUGCUUUGCCAUUA |
| BMPR-II | ON-TARGET plus SMARTpool, mouse BMPR-II (L-040599-00-0005; Thermo Fisher Scientific and GE Healthcare) | GCACAUAGGUCCCAAGAAA GAACGCAACCUGUCACAUA GCAUGAACCUUUACUGAGA CUAAUAAGCUAGAUCCAAA |
| β1 integrin | ON-TARGET plus SMARTpool, mouse ITGB1 (L-040783-01-0005; Thermo Fisher Scientific and GE Healthcare) | UGCCAAAUCUUGCGGAGAA UUACAAGAGUGCCGUGACA GUGAAGACAUGGACGCUUA CAAUGAAGCUAUCGUGCAU |
| β3 integrin | ON-TARGET plus SMARTpool, mouse ITGB3 (L-040746-01-0005; Thermo Fisher Scientific and GE Healthcare) | AAACAGAGCGUGUCCCGUA AAACACGUGCUGACGCUAA GAGCAGUCUUUCACUAUCA GUGAAAGAGCUGACGGAUA |
| Src | ON-TARGET plus SMARTpool, mouse Src (L-040877-00-0005; Thermo Fisher Scientific and GE Healthcare) | GCACGGGACAGACCGGUUA GGGAGCGGCUGCAGAUUGU UCAGAUCGCUUCAGGCAUG GCUCGUGGCUUACUACUCC |
| FAK | ON-TARGET plus SMARTpool, mouse Ptk2 (L-041099-00-0005; Thermo Fisher Scientific and GE Healthcare) | GAAGUUGGGUUGUUUGGAA GGGCAUCAUUCAGAAGAUA GCUCCAGAGUCAAUCAAUU GUACAGCACUCGCGUAUCU |
| Ilk | ON-TARGET plus SMARTpool, mouse ILK (L-040115-00-0005; Thermo Fisher Scientific and GE Healthcare) | GGACAUUGCACAAGGCCUA GCGCUUACAGAGUAUAUGA GAAGAUUCCUGUGUAUAGG GAACUUUGGUGGGAAAUGA |
| Cdc42 | ON-TARGET plus SMARTpool, mouse Cdc42 (L-043087-00-0005; Thermo Fisher Scientific and GE Healthcare) | GACUACGACCGCUAAGUUA CGGAAUAUGUACCAACUGU GAUGACCCCUCUACUAUUG AAACAGAAGCCUAUUACUC |
| Rock1 | ON-TARGET plus SMARTpool, Mouse Rock1 (L-046504-00-0005; Thermo Fisher Scientific and GE Healthcare) | GCACCAAUCUAUCGAAGAG UGUCGAAGAUGCCAUGUUA GACCUUCAAGCACGAAUUA GCGGUUAGAACAAGAAGUA |
| Rock2 | ON-TARGET plus SMARTpool, mouse Rock2 (L-040429-00-0005; Thermo Fisher Scientific and GE Healthcare) | GAGAUUACCUUACGGAAAA GCAAUGAAGCUUCUUAGUA CACAACAGAUGAUCAAAUA GGACAUGAGUUUAUUCCUA |
| FN | ON-TARGET plus SMARTpool, mouse FN (L-043446-01-0005; Thermo Fisher Scientific and GE Healthcare) | AGAACAAACACUAACGUAA GGUCAUUUCAGAUGCGAUU GGAGAGAGAUGCACCGAUU GGUUCAGACUCGAGGCGGA |

Table S4. **List of primer sequences for BMP receptors, FN, and collagen as well as for ATP50**

| Gene target | Primer sequences (5′ to 3′) |
|---|---|
| BMPR-Ia | Forward: TGCAAGGATTCACCGAAA; reverse: TGCTGCCATCAAAGAACG |
| BMPR-II | Forward: TTGGGATAGGTGAGAGTCGAAT; reverse: TGTTTCACAAGATTGATGTCCCC |
| FN | Forward: GCAGTGACCACCATTCCTG; reverse: GGTAGCCAGTGAGCTGAACAC |
| Collagen | Forward: TGTGTGCGATGACGTGCAAT; reverse: GGGTCCCTCGACTCCTACA |
| ATP50 | Forward: CTATGCAACCGCCCTGTACT; reverse: GATGATACCCTGGGTGTTGC |

# References


Pelish, H.E., J.R. Peterson, S.B. Salvarezza, E. Rodriguez-Boulan, J.-L. Chen, M. Stamnes, E. Macia, Y. Feng, M.D. Shair, and T. Kirchhausen. 2006. Secramine inhibits Cdc42-dependent functions in cells and Cdc42 activation in vitro. *Nat. Chem. Biol.* 2:39–46. http://dx.doi.org/10.1038/nchembio751

Prudent, R., E. Vassal-Stermann, C.-H. Nguyen, C. Pillet, A. Martinez, C. Prunier, C. Barette, E. Soleilhac, O. Filhol, A. Beghin, et al. 2012. Pharmacological inhibition of LIM kinase stabilizes microtubules and inhibits neoplastic growth. *Cancer Res.* 72:4429–4439. http://dx.doi.org/10.1158/0008-5472.CAN-11-3342